Second Quarterly Report | *Covering the Period 14 August to 14 November 1965*

RESEARCH ON COLD CATHODES

By: D. V. GEPPERT B. V. DORE

Prepared for:

NATIONAL AERONAUTICS AND SPACE ADMINISTRATION
GODDARD SPACE FLIGHT CENTER
GREENBELT, MARYLAND

GPO PRICE $ _____

CFSTI PRICE(S) $ _____

Hard copy (HC) $ 3.00

Microfiche (MF) .75

ff 653 July 65

CONTRACT NAS 5-9581

STANFORD RESEARCH INSTITUTE

MENLO PARK, CALIFORNIA

STANFORD RESEARCH INSTITUTE
MENLO PARK, CALIFORNIA

November 1965

Second Quarterly Report | *Covering the Period 14 August to 14 November 1965*

RESEARCH ON COLD CATHODES

Prepared for:

NATIONAL AERONAUTICS AND SPACE ADMINISTRATION
GODDARD SPACE FLIGHT CENTER
GREENBELT, MARYLAND

CONTRACT NAS 5-9581

By: D. V. GEPPERT B. V. DORE

SRI Project 5511

Approved: PHILIP J. RICE, MANAGER
PHYSICAL ELECTRONICS LABORATORY

J. D. NOE, EXECUTIVE DIRECTOR
ENGINEERING SCIENCES AND INDUSTRIAL DEVELOPMENT

Copy No. 11

ABSTRACT

GaP/W surface barrier diodes were fabricated in an oil-free high-vacuum system. Current-voltage, $1/C^2$ vs. V, and hot-electron data were obtained on these diodes. The results indicate a barrier height of 1.42 eV, with indications of some non-uniformity in barrier height over the diode area.

The work function of evaporated BaO on evaporated W was measured to be about 1.45 eV. There are indications that the BaO film condenses non-uniformly so that about 15 monolayers are required for complete coverage. Scattering of photo-excited electrons in the BaO film appears to set in at about 30 monolayers.

Theoretical studies have been conducted on BaO evaporation and on metal/semiconductor barriers as influenced by interfacial layers. An alternative cold cathode approach is suggested.

CONTENTS

ILLUSTRATIONS

TABLES

I INTRODUCTION

The objective of this program is to perform research on semiconductor/metal, hot-electron cold cathodes. The hot electrons are generated in a thin metal surface film by forward-biasing a rectifying semiconductor/metal diode. The metal film is on the order of 50-to-100 Å in thickness and is activated by a low-work-function coating to reduce the vacuum barrier below the semiconductor/metal barrier. Energy diagrams for the cathode, with and without bias, are shown in Figs. 1(a) and 1(b). The dimensions of the structure are not drawn to scale. The thickness of the metal film is exaggerated for reasons of clarity. Referring to Fig. 1(b), a portion of the hot electrons emitted over the top of the barrier into the metal film traverse the film ballistically and enter the vacuum. Most of the electrons that become scattered in the metal film are lost, however, and these electrons create a bias current for the device.

In our previous report, it was concluded that gallium phosphide (GaP) had good qualities for the semiconductor in fabrication of the surface-barrier cold cathode, where used with lead or alloyed tellurium-doped silver for the ohmic contact and platinum for the surface film. Because barium oxide (BaO)-activated platinum has a higher work function than the GaP/platinum surface barrier, however, other solutions were suggested. Long life and stability for low-work-function evaporated BaO surfaces were demonstrated in an ultra-high vacuum environment. The theory of metal/semiconductor contacts was extended and refined.

The steps which this report will concern itself with are:

1. Fabrication and testing of GaP/Tungsten surface barrier diodes.
2. Fabrication and testing of Tungsten/Barium Oxide phototubes.
3. Possible fabrication and testing of a surface-barrier cold cathode using the stated combination of materials.

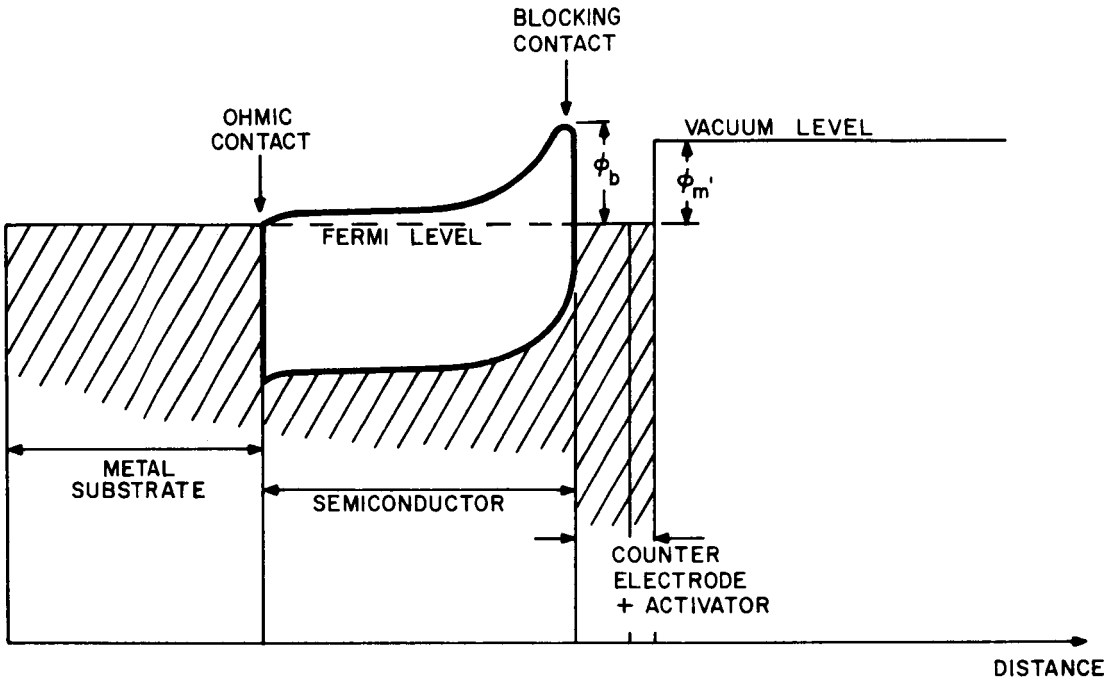

(a) ENERGY VS. DISTANCE OF SURFACE BARRIER CATHODE WITHOUT BIAS.

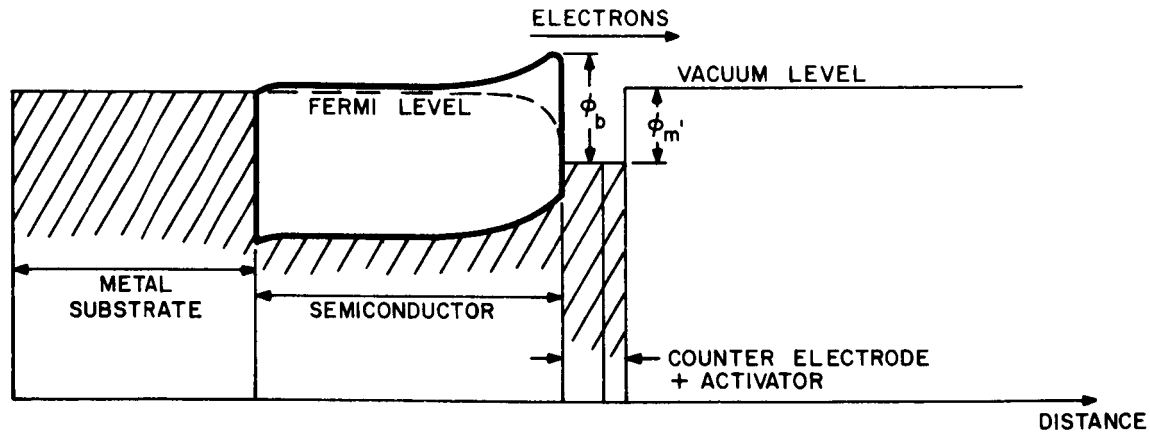

(b) ENERGY VS. DISTANCE OF SURFACE BARRIER CATHODE WITH BIAS.

FIG. 1 ENERGY DIAGRAM OF SURFACE BARRIER CATHODE

4. Continuation of life tests on the GaP/Platinum diode and on BaO phototubes.

II DISCUSSION

A. GaP/TUNGSTEN DIODES

1. Experimental Procedures

Gallium phosphide/tungsten surface barrier diodes were fabricated by evaporating tungsten (W) in an oil-free high-vacuum system. The gallium phosphide (GaP) crystal surfaces were first prepared by etching in hot aqua regia. As noted in the First Quarterly Report,[1]* this etch produces a mirror finish on one of the ⟨111⟩ crystal faces and a matte finish on the other crystal face. Lead (Pb) was alloyed to the side having the matte finish to produce an ohmic contact. The crystal was re-etched, and the acid was quenched with electronic grade methanol. The crystal was placed in the vacuum chamber wet with methanol. A mask was used for the W evaporation so as to produce three circular diode areas on the smooth crystal surface.

The system was given a good bake-out, after which the pressure was between 10^{-8} and 10^{-9} torr. A tungsten charge was heated by electron-beam bombardment up to evaporation temperatures, and a few hundred Å of W was evaporated.

2. Current-Voltage Characteristics

Using a tungsten probe to contact the circular evaporated-W areas, the current-voltage characteristics of the three diodes were examined. The diodes were first examined by means of a curve tracer. One of the diodes was found to be a poor rectifier and was therefore not examined further. The other two diodes appeared to be excellent rectifiers, as shown by the photograph of the trace reproduced in Fig. 2. The forward current does not become appreciable until a forward voltage of one volt is exceeded, indicating a barrier somewhat higher than one volt.

Accurate I-V data were then taken on one of the two good diodes, using two HP Model 425-A meters to read the current and the voltage.

*All references are listed at the end of the report.

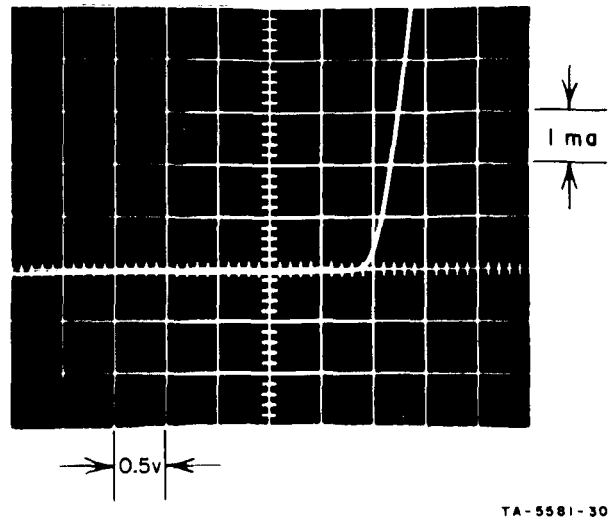

FIG. 2 I-V CHARACTERISTIC OF GaP/EVAPORATED W DIODE

Figure 3 is a plot of the I-V data on semi-log scales. These data have been corrected for the current flow through the 10^7 ohm input resistance of the voltmeter. The current is seen to increase exponentially with voltage over at least 4 decades of current. The current in this region follows the relation

$$I = I_o \, e^{\frac{qV}{nkT}} \qquad (1)$$

where n is about 1.7. For an ideal Schottky barrier, n should be equal to unity. The diode, therefore, does not follow simple Schottky theory. We note, however, that these diodes have a much lower value of n than the GaP/Pt diodes prepared earlier in an oil-diffusion-pumped system (as reported in the First Quarterly Report).[1] The high value of n for the GaP/Pt diodes (about 3.5) was attributed, at least in part, to a contaminating oil film between the GaP surface and the Pt film. This supposition seems even more reasonable now in view of the lower value of n found for a diode fabricated in an oil-free vacuum system. The different metals used in the two cases could, however, presumably also cause a different value of n.

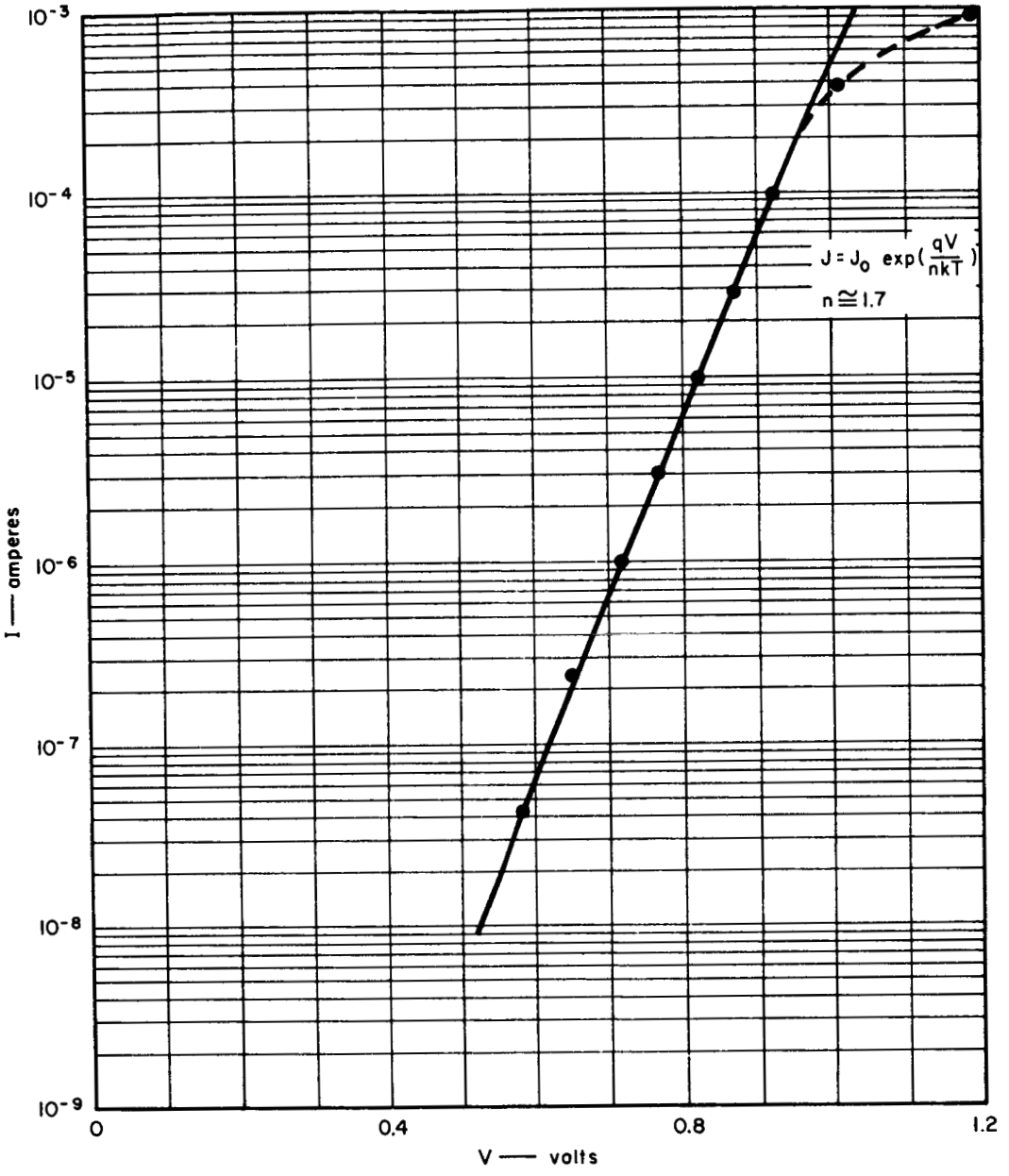

FIG. 3 LOG I vs. V PLOT FOR GaP/EVAPORATED W DIODE

The deviation of the current from the exponential rise above one volt is probably caused by the lateral resistance drop in the W film. Large lateral current flows are a natural consequence of using a simple point contact to the film made by the tungsten probe. The lateral film resistance can be estimated from the deviation noted to be about 200 ohms.

3. $1/C^2$ vs. V Data

The small-signal ac capacitance, C, of the barrier on one of the two good GaP/W diodes was measured as a function of dc bias voltage. A plot of $1/C^2$ vs. V is shown in Fig. 4. The voltage-axis intercept is about 1.5 volts, thus indicating a barrier height equal to, or perhaps slightly less, than this value. As will be pointed out in Sec. II-C-2, an interfacial layer between the semiconductor surface and the metal film can cause a larger voltage-axis intercept V_o than the true diffusion potential

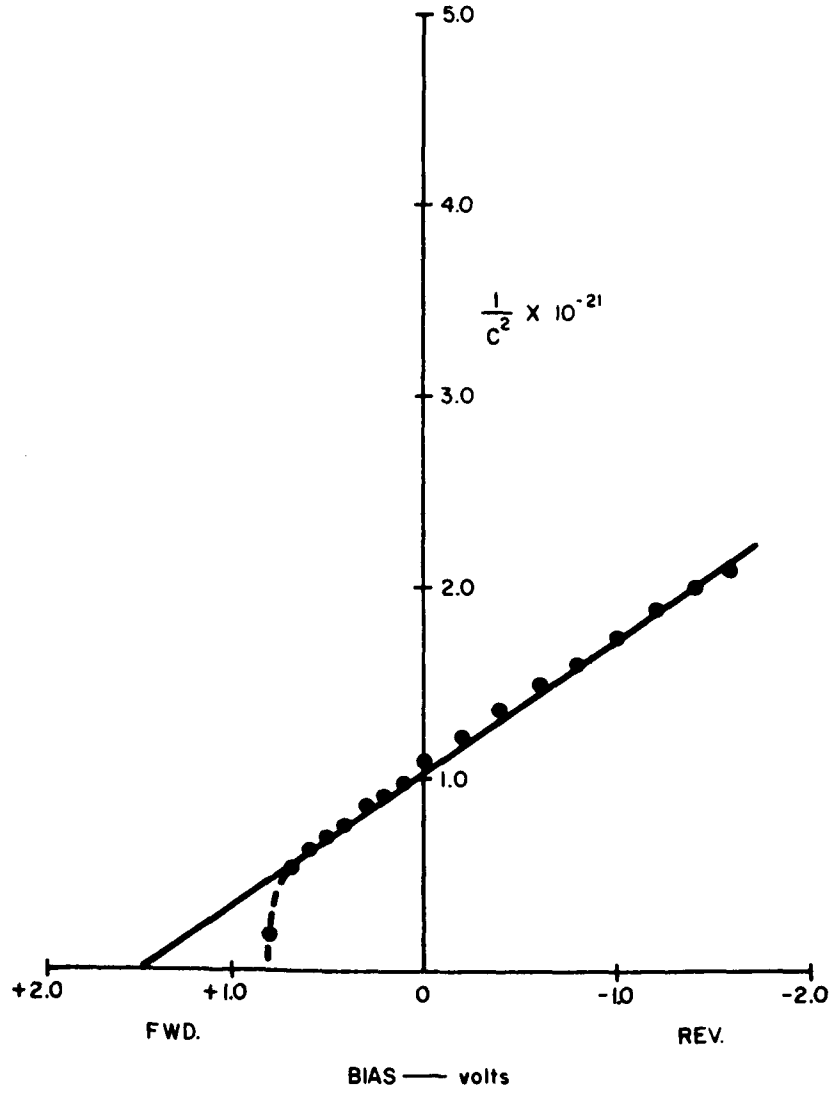

FIG. 4 $1/C^2$ vs. V FOR GaP/EVAPORATED W DIODE

V_{BO} of the barrier, with the larger values of V_o corresponding to thicker interfacial layers. In the First Quarterly Report, $1/C^2$ vs. V data were presented for GaP/Pt diodes prepared in an oil-diffusion-pumped vacuum system.[1]* The values of V_o found for these diodes was between 3 and 4 volts, indicating a relatively thick interfacial film of pump oil. The GaP/W diodes under discussion now were prepared in an oil-free vacuum system, and the low value of V_o shown in Fig. 4 indicates little or no interfacial contamination. This subject is treated in detail in Appendix B.

In the forward direction the $1/C^2$ curve appears to go to zero at about 0.8 volts. The simplest explanation for this is that a small area of the diode has a low barrier of about 0.8 eV whose capacitance therefore approaches infinity as the bias approaches +0.8 volts. The uniformity of the barrier over the area of the diode is of great importance for the operation of the cathode. Consider a diode having a continuously-distributed range of barrier heights. At low forward biases, essentially all the forward current will be carried by those areas having the lowest barrier height. The hot electrons generated by these low barriers might well be below the vacuum energy level, and the emission efficiency at low bias levels might therefore be very low. Fortunately, as the bias is increased, the current flowing through the low-barrier areas will become series-resistance-limited, so that a larger proportion of hot electrons to "warm" electrons would be generated. The emission efficiency would thus increase rapidly with increasing bias, so that at high bias levels the efficiency might not suffer significantly from barrier nonuniformities.

It can even be speculated that the deviation of the I-V characteristics from ideal Schottky theory is a simple consequence of barrier height nonuniformity. In Fig. 3, for instance, the current increased exponentially with voltage, but with a coefficient that was too low by a factor of 1.7. Such behavior would be qualitatively consistent with a continuously-distributed range of barrier heights.

---

*See Figs. 12 and 13, p. 26.

Further evidence of barrier-height nonuniformity will be presented in the following section.

4. Hot-Electron Data

One of the two good GaP/W diodes was mounted at the focus of an elliptical mirror positioned to focus the light from the exit port of a PE112 spectrometer. Contact to the tungsten film was made with a gold wire spring probe, and the diode was mounted on an x-y-z micropositioner so that the photovoltaic response could readily be maximized. Figure 5 shows a plot of the square root of the photovoltage $\sqrt{R}$ vs. the photon energy. Extrapolation of the straight line portion of the curve to the energy axis yields an intercept of 1.42 eV, thus indicating a barrier height of this magnitude. This value is considered to be more accurate than the value of 1.5 eV obtained from the $1/C^2$ vs. V plot, and it is within the experimental error of the latter.

The cause for the maximum and minimum photovoltage observed in the plot at values of $h\nu$ equal to about 2.15 eV and 2.25 eV, respectively, is not understood at the present time. The deviation from the straight-line region observed for photon energies less than about 1.55 eV can be understood very simply in terms of a nonuniform barrier height, as discussed previously. In fact, the size of the "tail" can be interpreted in terms of the relative magnitudes of the areas having barrier heights lower than 1.42 eV. It would appear, if this interpretation is correct, that most of the diode area--say 80 to 90 percent--has a barrier height of 1.42 eV. This leaves perhaps 10 to 20 percent of the area having barriers ranging from 1.42 eV down to perhaps 0.8 eV (as determined by the $1/C^2$ vs. V plot).

B. WORK FUNCTION OF TUNGSTEN/BaO

1. Experimental Procedure

When we found that vacuum barriers below 1.5 eV could not be obtained by activating evaporated Pt films with BaO,[1] it was decided to use W in place of the Pt. The procedure in activating with BaO has been described in previous reports. At least one significant change has been made, however.

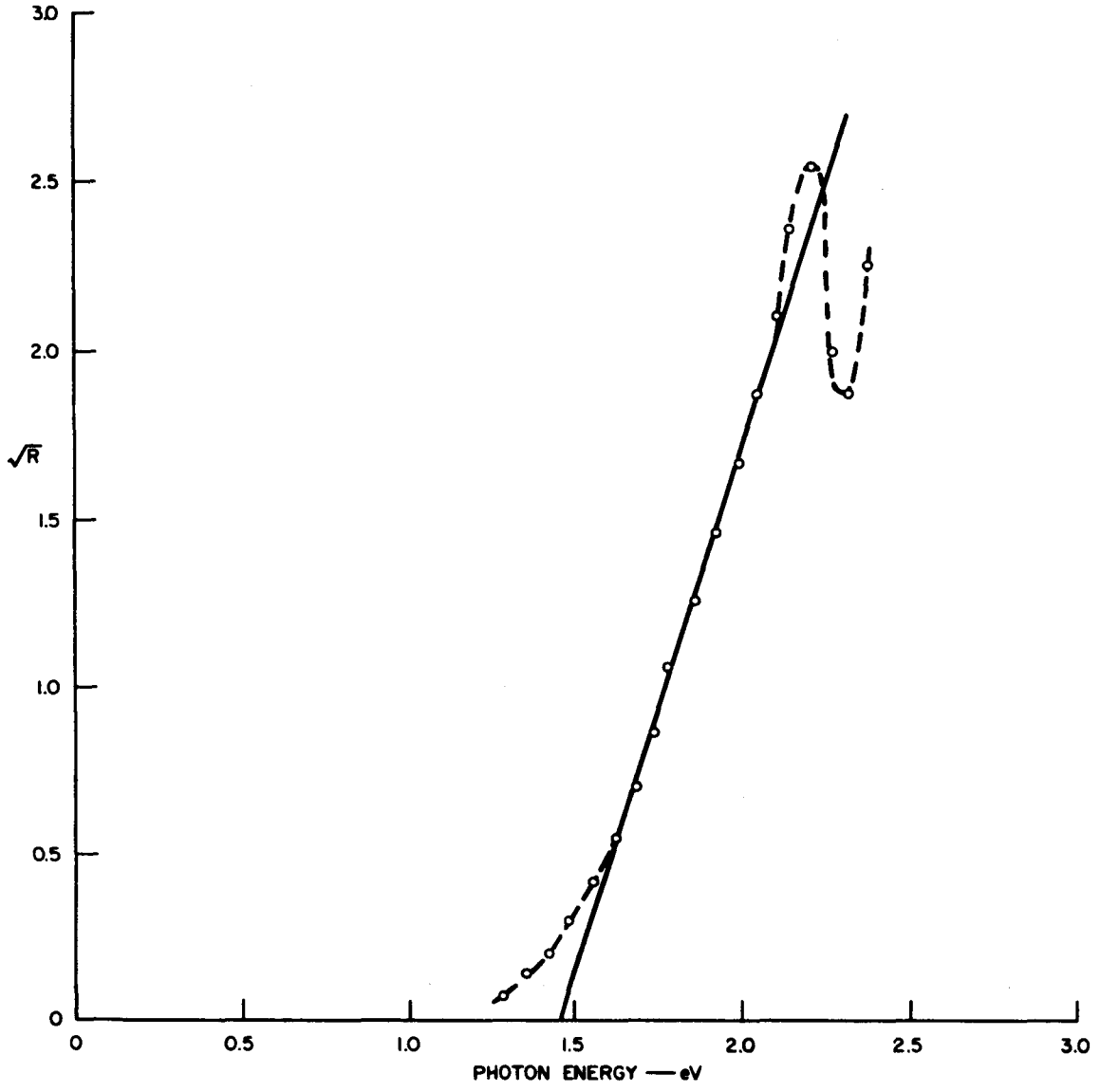

FIG. 5 SQUARE ROOT OF PHOTORESPONSE vs. PHOTON ENERGY FOR GaP/W DIODE

It was previously thought a rapid evaporation of BaO would result in the liberation of free Ba, which could be detrimental. An analysis of the evaporation process is included as Appendix A to this report. It was performed by Dr. Cubiocciotti, a Scientific Fellow in the Physical Sciences Division at the Institute. This analysis indicates free Ba can be produced in the reaction of BaO with refractory metal heaters such as W and Mo. In addition, the oxides of those refractories

are produced, which would increase the value of the work function of the surface. When a Pt heater is used for the source, however, these effects are considerably reduced or completely absent.

In the experiments that follow, Pt heaters were used at a temperature of 1100° C. As a result the evaporation rate was about one monolayer per minute, which is much more rapid than obtained previously. This procedure has the advantage of reducing the amount of gas occluded in the BaO film during deposition.

2. Run No. 1

This experiment was set up to accomplish several objectives:

a. To form a GaP/W diode and to confirm the height of the metal/semiconductor barrier.
b. To activate the W with BaO and measure the height of the vacuum barrier.
c. To obtain electron emission by applying forward bias to the diode, if the barriers measured in (a) and (b) were compatible.

A GaP crystal, with preformed ohmic contacts of Ag-Te on one side and evaporated Pt contact areas on the other side, was mounted on a rotating assembly in the oil-free vacuum system. We planned to evaporate approximately 100 Å of W by monitoring the resistance across the Pt contacts during the evaporation. The film deposited was several hundred Angstroms in thickness, however, because of intermittent electrical contact to the rotating assembly. The GaP/W barrier could not be measured photoelectrically with such a thick W film, so the BaO activation was started after rotating the crystal assembly approximately 45° to face the BaO source. Very little photosensitivity was obtained, and the presence of water vapor in the vacuum system was suspected due to an insufficient bake-out. When the Pt filament in the BaO source burned out the experiment was terminated.

Although none of the objectives were achieved in this experiment, good GaP/W-Pt diode characteristics were obtained with no indication of deterioration in vacuum, as was the case with polycrystalline TiO_2.

3. Run No. 2

Another experiment was then constructed to measure only the vacuum barrier of BaO-activated W. A substrate of hydrogen-fired sheet Mo was placed at a 45° angle to the viewing part so that optical measurements could be made. A rotating shutter controlled by an external magnet was used to shield the substrate during the conversion of the $BaCO_3$ to BaO. A circular deposit of W was evaporated on to the Mo, but a short developed in the electron gun before a thick film could be deposited. BaO was then evaporated until a maximum photosensitivity was obtained.

The light was not restricted to the W area because the work function of BaO on sheet Mo had been measured previously as 1.75 to 1.80 eV, and if the value for W was in the vicinity of 1.4 eV, it could be distinguished from the Mo/BaO response. When a single value of 1.86 eV was obtained with no indication of a lower intercept, it was concluded that there was insufficient W evaporated.

The need for a good vacuum to form and maintain a low work function surface with BaO has been acknowledged. Some indication of the quality of the vacuum required was obtained in this experiment. A pressure of 1.4×10^{-9} torr was observed at the pump during the work function measurements. Based upon subsequent measurements with a Redhead Magnetron gauge coupled to the experimental chamber, the actual vacuum in the region of the cathode was estimated to be in the $6\text{-}8 \times 10^{-9}$ torr range. During the evaporation of the BaO the pressure probably rose to the vicinity of 5×10^{-8} torr.

A plot of the peak photoelectric response vs. time in hours for the BaO on Mo is shown in Fig. 6. This is interesting but not too meaningful as the photon energy at the peak also shifted with time. A series of $\sqrt{R}$ vs. photon energy plots were made from the data to obtain a measure of the degradation in work function with time. As shown in Fig. 7, it increased from 1.86 eV to 2.5 eV in 24 hours.

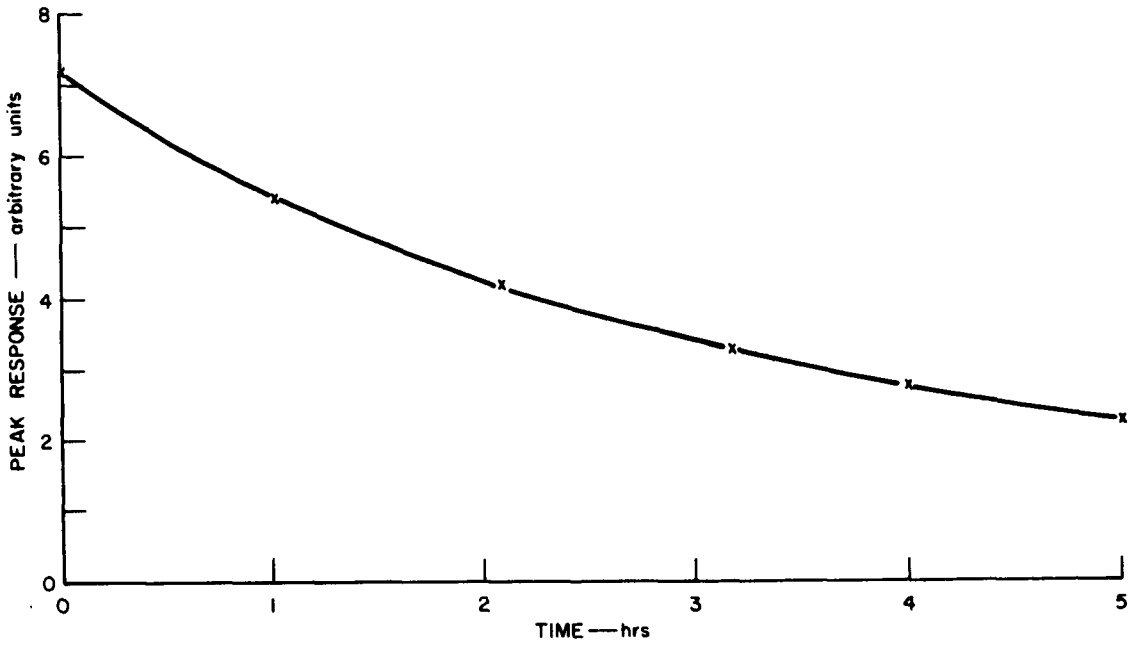

FIG. 6 PLOT OF PEAK PHOTORESPONSE OF W/BaO vs. TIME (Run #2)

Assuming a sticking factor of 0.10 on the surface of the Ba , a monolayer of the residual air will form on the surface in approximately 6.5 hours at a pressure of 7×10^{-9} torr. By this time the work function had increased 0.36 eV.

4. Run No. 3

The experiment described in Run #2 did not provide any information on the activation of evaporated W with BaO, so we repeated it with a thicker deposit of W on the Mo substrate. The BaO was applied in a series of 5 minute evaporations. After each evaporation a recording was made of the spectral response. These results were plotted up in a set of $\sqrt{R}$ vs. $h\nu$ curves shown in Fig. 8a, 8b, and 8c. The work functions obtained from the intercepts of these curves are plotted as a function of accumulated deposition time in Fig. 9.

A value of 4.36 eV from Suhrmann and Wedler[2] was used for the work function of the freshly evaporated W. More readings should have been taken in the first five-minute interval, but the values obtained after 5 and 10 minutes of evaporation indicate the same sort of

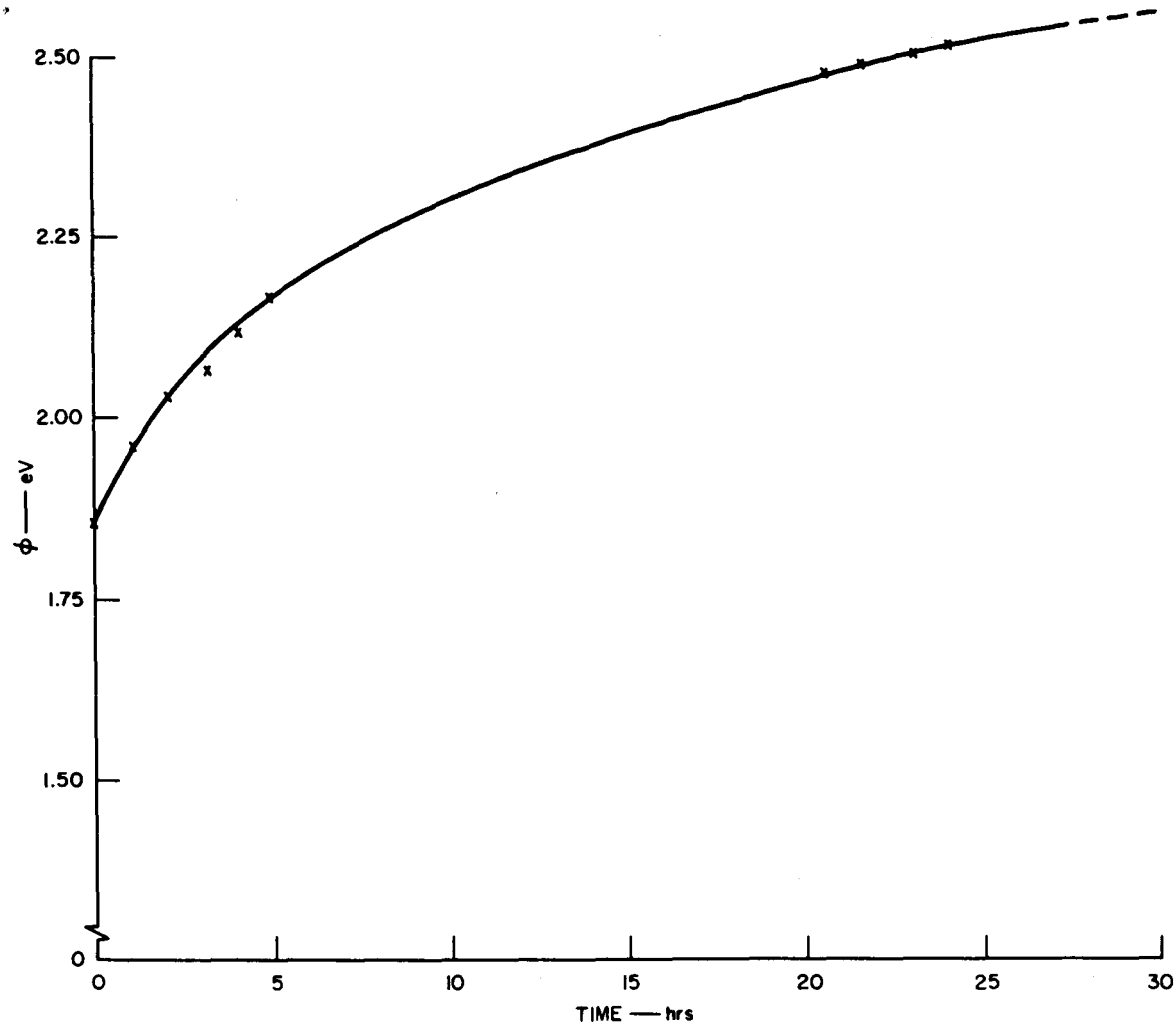

FIG. 7 PLOT OF WORK FUNCTION OF W/BaO vs. TIME (Run #2)

inflection in the value of φ observed by Moore and Allison[3] in the early stages of the activation.

Optimum activation occurred after 30 minutes of evaporation. Referring again to the results of Moore and Allison[3], we infer the thickness of the BaO deposit was in the range of 20-30 monolayers. Continuing the evaporation for another 5 minutes resulted in the slight increase in φ that has been observed by other investigators.[4] The lower response obtained after 35 minutes evaporation time (Fig. 8c) indicates some scattering of photo-excited electrons in the BaO film. For still thicker BaO films the photoelectric response would ultimately approach that of bulk BaO.

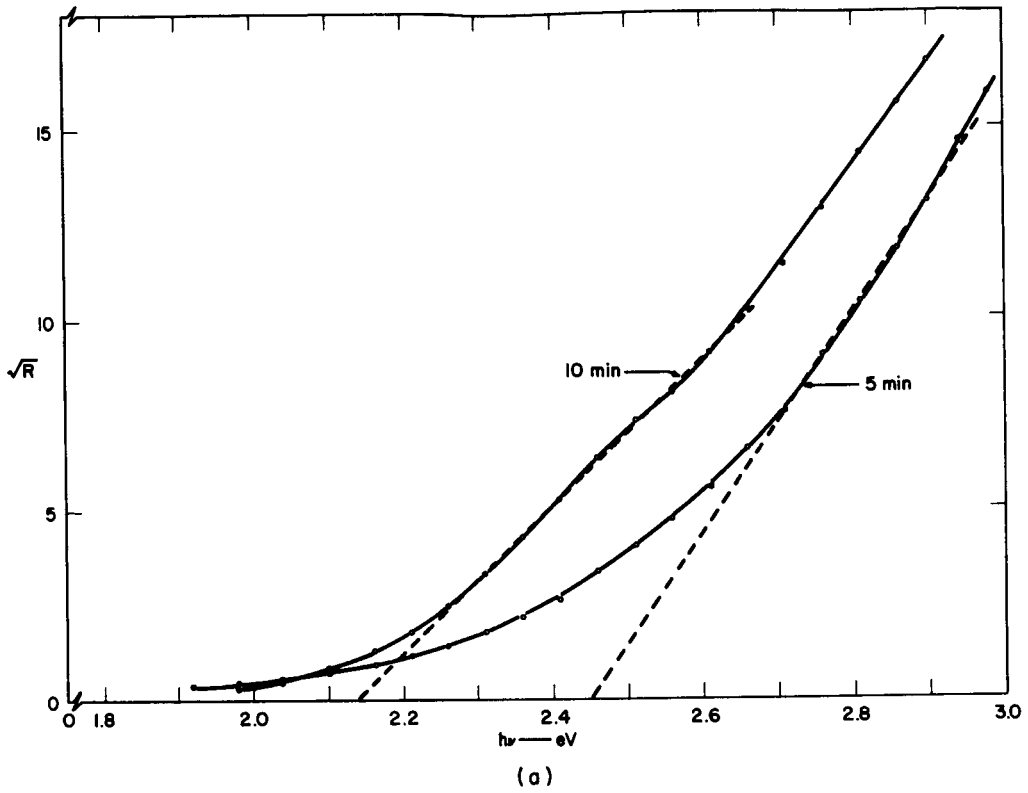

(a)

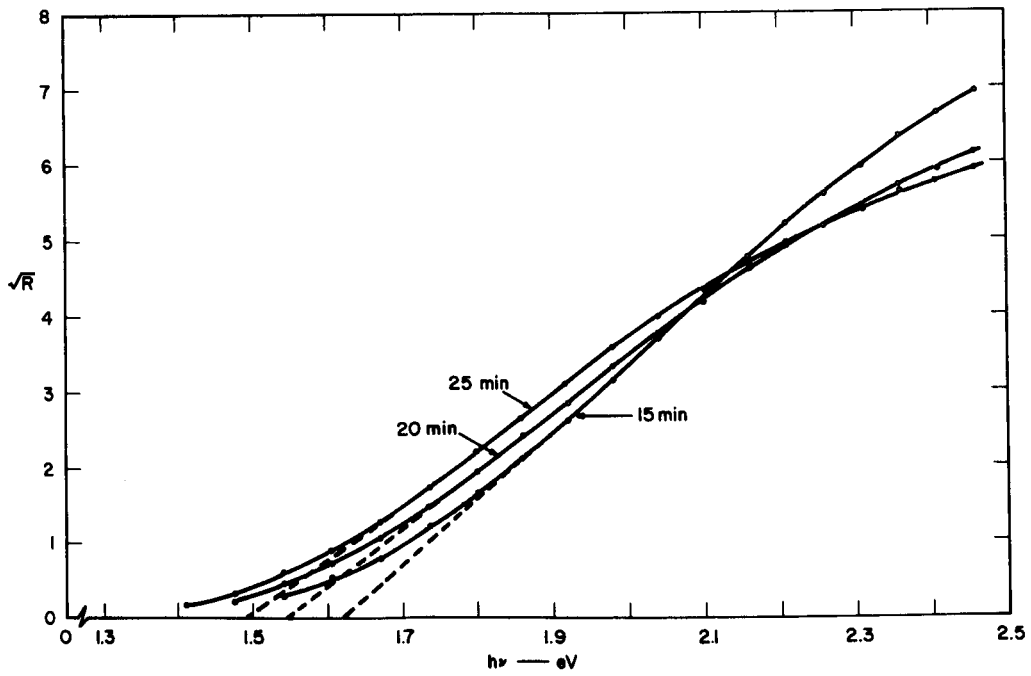

(b)

FIG. 8 SUCCESSIVE PLOTS OF SQUARE ROOT OF PHOTORESPONSE vs. PHOTON ENERGY DURING ACTIVATION OF EVAPORATED W WITH BaO (Run #3)

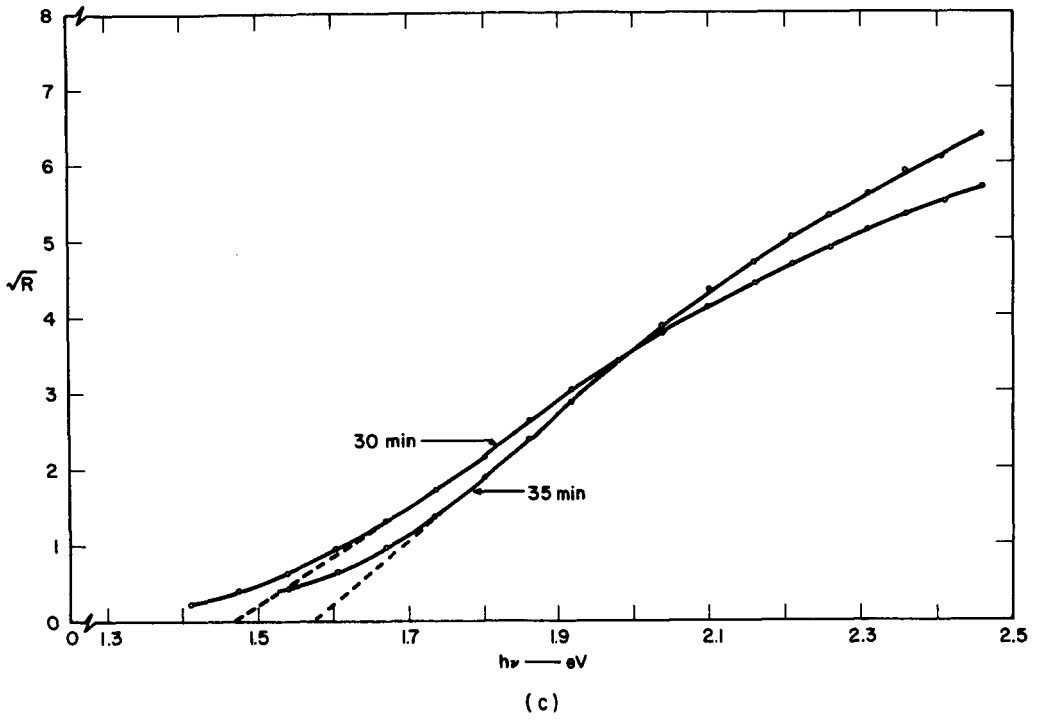

(c)

FIG. 8 Concluded

Figure 10 is a Fowler plot of the response obtained with optimum activation. This yields a value of 1.39 eV, while the $\sqrt{R}$ vs. hν plot yields 1.47 eV. Considering the inherent inaccuracies in making the measurements and interpreting the results, the most probably value for the work function of the W/BaO surface is 1.45 eV. This is only 0.03 eV higher than the GaP/W barrier reported in Sec. II-A-4. It is therefore likely a GaP/W/BaO cathode structure will emit, although the efficiency might be low.

It is interesting to note that the curves for 5 and 10 minute evaporation times (Fig. 8a) are concave upward. This is quite possibly an indication the BaO is not condensing on the substrate as a uniform, continuous layer. As the evaporation is continued, a more uniform work function over the surface area is obtained, yielding the more nearly linear plots shown in Figs. 8b and 8c. Thus, it would appear a continuous BaO film is only obtained for films on the order of 10 to 15 monolayers thick.

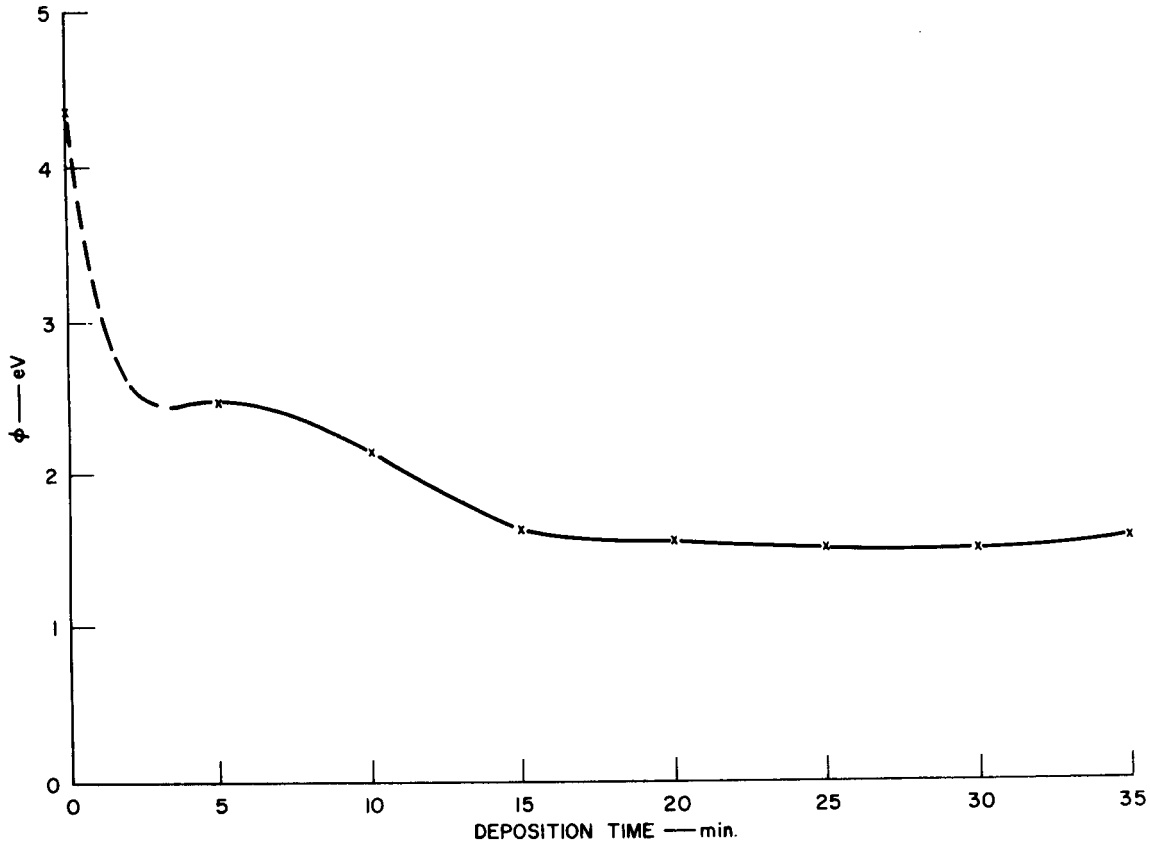

FIG. 9 PLOT OF WORK FUNCTION vs. DEPOSITION TIME FOR W/BaO (Run #3)

C. THEORETICAL CONSIDERATIONS

1. BaO Evaporation*

A considerable amount of information of evaporating BaO has been published since Moore and Allison's paper[3] in 1950. Some of this literature has been reviewed, and a few significant points are summarized below. A table (Table I) of minimum values of work functions has also been prepared. This table includes the method of measurement and some information on preparation.

a. Russel and Eisenstein[6] measured evaporation rates using a radioactive tracer, $Ba^{140}CO_3$. With the source at 1310° K, they deposited

*This section is reproduced from the First Interim Report on Contract DA-44-009 AMC-1206(T).[5]

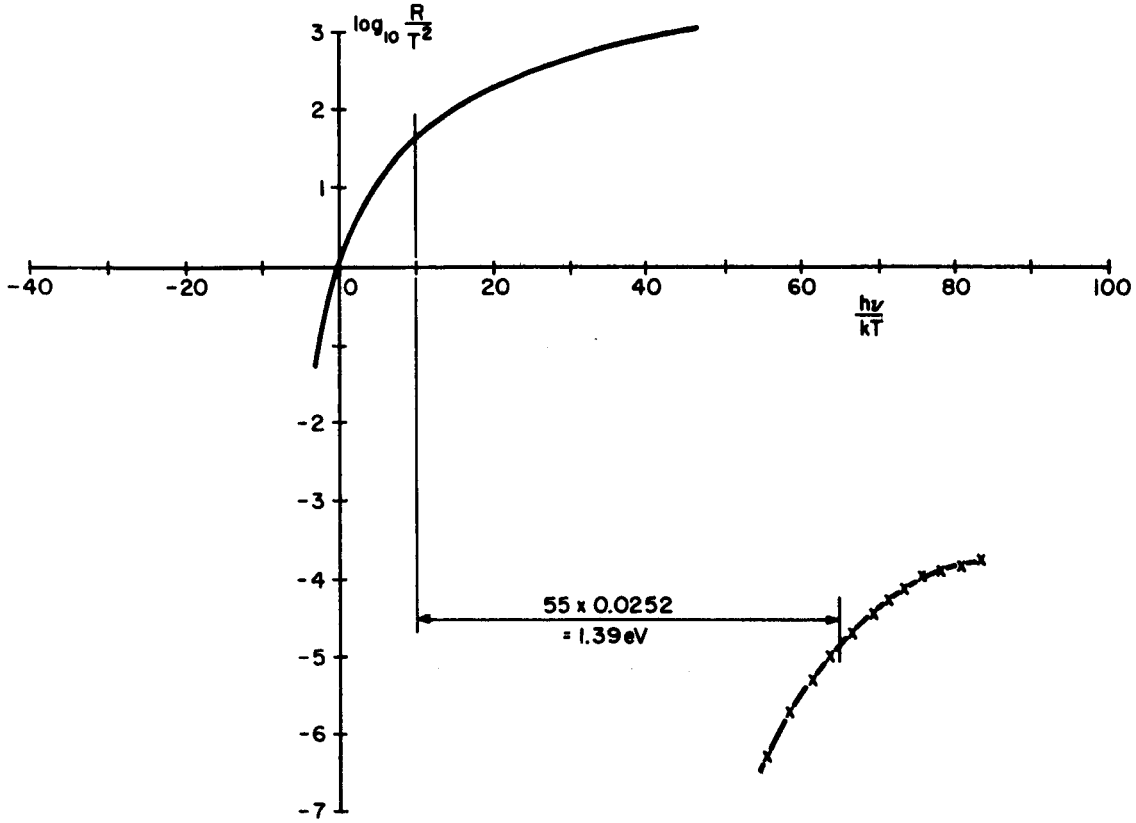

FIG. 10 FOWLER PLOT FOR W/BaO PHOTOTUBE WITH OPTIMUM ACTIVATION

Table I

BaO ACTIVATION RESULTS

Substrate	Minimum Work Function (eV)	Type of Measurement	Remarks	Reference
Mo	1.0	Thermionic	10-30 monolayers	Moore and Allison[3]
Mo	1.2	Thermionic	1 monolayer	Moore and Allison[3]
W	1.1	Thermionic	10-30 Monolayers	Moore and Allison[3]
W	1.2	Thermionic	1 monolayer	Moore and Allison[3]
Ta	1.0	Thermionic	10-30 monolayers	Moore and Allison[3]
Ta	1.3	Thermionic	1 monolayer	Moore and Allison[3]
Ni	1.27	Thermionic	27 monolayers with Ni substrate at 800° K	Russel and Eisenstein[6]
W	2.0	Retarding potential	Electric field applied during evaporation	Hopkins and Ross[7]
Mo	1.0	Thermionic	Relatively thick deposits. Different types of measurements made on same cathode	Narita[8]
	1.70	Photoelectric		
Ta	1.20	Thermionic		
	1.69	Photoelectric		
Mo	~1.7*	Retarding potential	Obtained in 10 secs with source at 1223° K	Florio[9]
Mo	~1.25*	Contact potential difference	Mo substrate heated to 1270° K during deposition	Kirsanova and Shul'man[10]
Evaporated Ni	~1.5*	Not specified, but most likely retarding potential measurements	Measurements made with substrates at 78° K	Ptushinskii[11]
Evaporated W	~1.4			
Evaporated Cu	~2.1			
Evaporated Ge	~1.6			
W foil	~1.65*	Contact potential difference	W substrate at 1100° K; very slow deposition rate	Kirsanova, Shul'man and Dement'eva[4]

*Work function values for the last four references were read from graphs.

one monolayer in 27 minutes through a 5-mm aperture with a source-to-substrate spacing of 7 mm. They report the rate doubles for each 15 degrees increase in temperature.

b. Russel and Eisenstein[6] also observed the effects heating the substrate had upon the structure of the BaO deposit. With a polished Ni substrate heated to 800° K, the films were crystalline when examined at room temperature. For substrate temperatures ≤ 450° K, the films were amorphous. When crystalline deposits were subsequently heated to 1070° K and higher, they returned to an amorphous state. A minimum thermionic work function at 1.27 eV was obtained for 27 monolayers of BaO deposited on the Ni substrate heated to 800° K.

c. Hopkins and Ross[7] measured a minimum work function of 2.0 eV for BaO on W by means of retarding potential plots. This result was obtained by applying 100 volts between the BaO source and the W substrate during evaporation. Without this field the work function was 0.8- to 1.0-eV higher. One possible interpretation is that the result was caused by the orientation of the BaO molecules on the W in the presence of the field.

d. Narita[8] measured the work function of BaO on Mo and Ta substrates thermionically and photoelectrically. For thin films of BaO there was good agreement between the two measurements, but the values of φ were of the order of 2.0 eV. For thicker films of BaO, the thermionic values approached 1.0 eV and were 0.5- to 0.7-eV lower than the photoelectric values.

e. Florio[9] describes a retarding-field technique for measuring the effect of evaporating BaO. This technique uses the current-voltage relation

$$I_r = sAT^2 \exp\left[-e(-V_a + \varphi_a)/kT\right] \quad ,$$

where I_r is the retarding field, V_a is the anode voltage, s is the emitter area, and

$$A = 120 \text{ amperes/cm}^2/\text{deg}^2 \quad (2)$$

Provided the source temperature, T, remains constant, the change in the applied voltage, V_a, necessary to maintain a constant value of I_r, is a measure of the decrease in the anode work function, φ_a. Using a constant current supply for the test diode, a continuous recording of the change in anode work function can be made.

f. Dueker and Hensley,[12] in a study of the energy distribution of the photoelectric emission from BaO, found the emission threshold was reduced by approximately 0.3 eV after applying 0.6 monolayer of Ba to the surface of the BaO cathode. They experimented with three types of BaO: thermal reduction of sprayed $BaCO_3$, oxidation of evaporated films of Ba, and evaporated films of BaO. They found that the evaporated BaO gave them the most satisfactory results.

2. Metal/Semiconductor Barriers

Barriers: The barrier height data for GaP/Pt, as published in the First Quarterly Report, will be interpreted here in detail. This will be based upon models suggested by Cowley.[13]

The fact the intercept of the $1/C^2$ plot for a metal/semiconductor junction is larger than the true diffusion potential when an interfacial layer is present has been pointed out by Goodman.[14] He derives an expression in terms of interfacial layer thicknesses for the difference between V_o, the $1/C^2$ intercept, and V_{BO}, the diffusion potential. This is based on the assumption that the amount of charge in surface states, if any, is independent of the applied bias. The dependence of V_{BO} on δ is not explicitley derived. For this reason, Goodman's expression may not be used to predict the magnitude of V_o as a function of δ for a particular metal/semiconductor system with all other parameters held fixed. The assumption that Q_{ss}, the surface states charge, is independent of bias is also open to question.

Cowley[13] has considered three models for the behavior with bias of the metal/semiconductor junction with an interfacial layer and surface states. The difference in the models involves the assumed behavior of the

charge in surface states when an applied bias is impressed. Referring to Fig. 11, the following relations for the metal/interfacial layer/semiconductor system, with and without bias, respectively, are valid:

$$\varphi_m + V = \varphi_n + V_B + E_A + \Delta \tag{3a}$$

$$\Delta = \frac{\delta}{\epsilon_i} \left\{ \left[2e\epsilon_s N_D (V_B - V_2) \right]^{1/2} + Q_{ss}(V) \right\} \text{ (Gauss' Law)} \quad . \tag{3b}$$

and

$$\varphi_m = \varphi_n + V_{BO} + E_A + \Delta_o \tag{4a}$$

$$\Delta_o = \frac{\delta}{\epsilon_i} \left\{ \left[2e\epsilon_s N_D (V_{BO} - V_2) \right]^{1/2} + Q_{ss}(0) \right\} \quad . \tag{4b}$$

where subscripted zeroes indicate the value of a quantity when no bias is applied. The important quantities in equations (3) and (4) are defined in Fig. 11. The V_2 term is the reserve layer correction and is ordinarily small, of the order of 30 mV. The assumptions for the different models regarding surface state dependence on bias can now be listed:

Model No. 1: For the case of an intimate metal/semiconductor contact (very thin interfacial film), it is assumed that the Fermi level at the semiconductor surface remains "pinned" to the Fermi level in the metal. In this case the change in surface-state charge when a bias is applied is given by

$$\Delta Q_{ss} = - eD_s (\Delta - \Delta_o) \quad . \tag{5}$$

Model No. 2: The assumption is made here that the change in the electron quasi-Fermi level at the semiconductor surface due to an applied bias is equal to the potential change across the interfacial film, in which case there will be no change in Q_{ss} with an

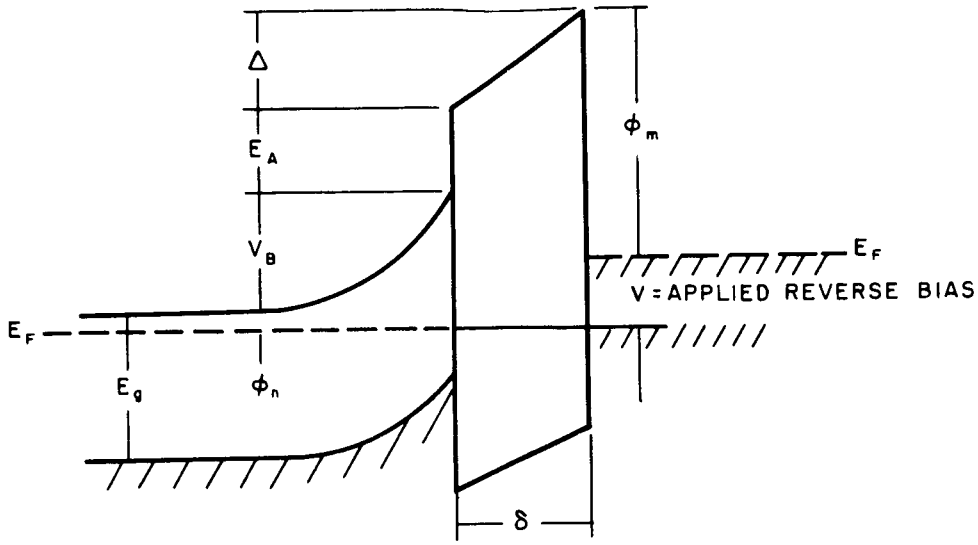

(a) METAL-SEMICONDUCTOR WITH APPLIED REVERSE BIAS

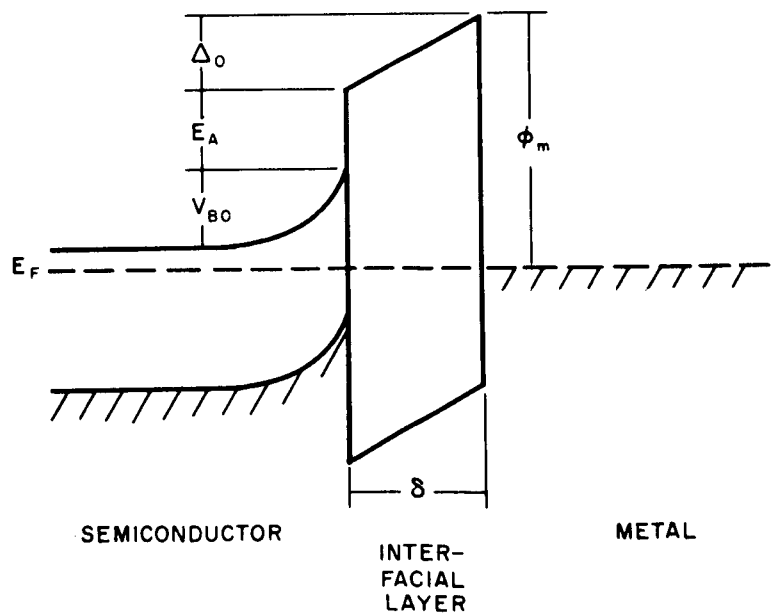

(b) METAL-SEMICONDUCTOR IN EQUILIBRIUM

FIG. 11 (a) METAL-SEMICONDUCTOR WITH APPLIED REVERSE BIAS
(b) METAL-SEMICONDUCTOR IN EQUILIBRIUM

applied bias. There is no a priori reason for assuming that Q_{ss} remains fixed when a bias is applied; in general, one expects that Q_{ss} will change with bias. The assumption of $\partial Q_{ss}/\partial V \equiv 0$ does, however, lead to a mathematically tractable model which in most cases will turn out to provide a useful approximation to the actual junction behavior.

Model No. 3: For thick interfacial layers, the Fermi level at the semiconductor surface will remain fixed at the Fermi level in the bulk semiconductor. This is the assumption usually made in field effect measurements of the surface-state density.[15,16] This model will not be used here, since the requirement for a thick ($\approx$ 1000 Å) film is obviously not fulfilled.

Analysis of Model No. 1:

We are ultimately interested in obtaining an expression for the depletion capacitance of the junction as a function of applied bias. The depletion capacitance is defined as the derivative of the charge entering one contact with respect to the applied voltage. Since for this model we are assuming that the surface Fermi level is pinned to the Fermi level in the metal, any change in surface-state charge is provided by the metal. Calculation of the depletion capacitance therefore involves taking the derivative of the semiconductor space charge Q_{sc} with respect to bias voltage V. The algebra for this calculation has been performed by Cowley and the result is

$$C = \left[\frac{e\epsilon_s N_D}{2}\right]^{1/2} \left[V + \frac{\varphi_{ms} + \alpha(E_g - \varphi_o - \varphi_n)}{1 + \alpha} + \frac{V_1}{4(1 + \alpha)^2} - V_2\right]^{-1/2}$$

$$\text{farads/m}^2 \quad \ldots \qquad (6)$$

where

$$\alpha = eD_s \frac{\delta}{\epsilon_i} \qquad (7)$$

$$V_1 = 2e\epsilon_s N_D \left(\frac{\delta}{\epsilon_i}\right)^2 \tag{8}$$

$$\varphi_{ms} = \varphi_m - (E_A + \varphi_n) \tag{9}$$

and D_s is the surface states density in states/cm^2/eV, regarded here as a constant. The expression for the capacitance is obtained by first using Eqs. (3), (4), and (5) to solve for $V_B - V_2$, and then using the relation

$$Q_{sc} = \left[2\epsilon_s e N_D \, (V_B - V_2)\right]^{1/2} \tag{10}$$

to obtain the space charge. Differentiation of Eq. (9) with respect to applied (reverse) bias V yields Eq. (6).

Squaring and inverting the capacitance relation Eq. (6) yields

$$\frac{1}{C^2} = \frac{2}{e\epsilon_s N_D} \left[V + \frac{\varphi_{ms} + \alpha(E_g - \varphi_o - \varphi_n)}{1 + \alpha} + \frac{V_1}{4(1 + \alpha)^2} - V_2\right] \quad . \tag{11}$$

The voltage-axis intercept of Eq. (11) is given by

$$V_o = -\left[\frac{\varphi_{ms} + \alpha(E_g - \varphi_o - \varphi_n)}{1 + \alpha} + \frac{V_1}{4(1 + \alpha)^2} - V_2\right] \quad . \tag{12}$$

Inspection of the GaP/Pt data in Figs. 12 and 13 of the First Quarterly Report[1] shows the value of V_o here is of the order of 3 to 4 eV, while the true value of V_{BO}, as determined from photothreshold measurements, is only about 1.4 eV. Cowley[13] has reported similar observations for GaP/Pt diodes prepared in an oil-diffusion vacuum station. In addition, Cowley reports that for GaP/Pt diodes prepared in a Vac-Ion vacuum station, close agreement was obtained between values of V_o and V_{BO}, and that $V_o \approx V_{BO} \approx 1.45$ eV. The difference in behavior between diodes prepared in the two vacuum stations can definitely be ascribed to the formation of a contaminating film, presumably diffusion pump oil, in the case of

the diodes prepared in the oil system.[17] A model which correctly describes this situation must therefore show V_o increasing rapidly with δ, the interfacial layer thickness, and should show V_{BO} changing much more slowly with δ. A detailed inspection of Eq. (12) reveals it approaches a limit as the interfacial layer thickness gets large. The limiting value of Eq. (12) is

$$\lim_{\delta \to \infty} V_o = - \left\{ \left(E_g - \varphi_o - \varphi_n \right) + \frac{\epsilon_s N_D}{2eD_s^2} - V_2 \right\} \quad . \tag{13}$$

For GaP/Pt, assuming $N_D \simeq 5 \times 10^{17}$ cm^{-3}, $D_s \simeq 3 \times 10^{13}$ cm^{-2} eV^{-1}, $\epsilon_s = 10\epsilon_o$, and $\varphi_o + \varphi_n \simeq \frac{1}{3} E_g$, according to Cowley and Sze[18] V_o has a limiting value of about 1.5 eV. This is clearly not in accord with experiment, since the observed value of V_o for GaP/Pt was between 3 and 4 volts. Furthermore, since the assumption upon which Model #1 is based is that δ is very small, it is not expected that the result of the above limiting process will be meaningful. We therefore conclude that while Model #1 might provide a correct description of the behavior of the diode capacitance for very thin interfacial layers, it cannot account for the very large values of V_o observed in the experiments described here. We will accordingly proceed to an analysis of Model #2.

Analysis of Model No. 2

In this model it will be assumed that the surface states charge Q_{ss} does not change with applied bias. This is admittedly not a physically reasonable assumption, but does lead in a straightforward manner to results which seem to approximate the observed behavior of V_{BO} and V_o with changes in interfacial layer thickness. The resulting expression for V_o from Cowley[18] is

$$V_o = - \left[V_{BO} - V_2 + \frac{V_1}{4} + V_1^{1/2} \left(V_{BO} - V_2 \right)^{1/2} \right] \tag{14}$$

where V_{BO} is given by

$$V_{BO} = \frac{\varphi_{ms} + \alpha(E_g - \varphi_o - \varphi_n)}{1 + \alpha} + \frac{V_1}{2(1 + \alpha)^2}$$

$$- \frac{1}{(1 + \alpha)^2} \left[(1 + \alpha) V_1 \{\varphi_{ms} + 2(E_g - \varphi_o - \varphi_n)\} + \frac{V_1^2}{4} \right]^{1/2} \tag{15}$$

The behavior of V_o in the limit of large δ can be seen as follows. V_{BO} tends to a finite limit:

$$\lim_{\delta \to \infty} V_{BO} = (E_g - \varphi_o - \varphi_n) + \frac{\epsilon_s N_D}{eD_s^2}$$

$$- \left[\left(\frac{\epsilon_s N_D}{eD_s^2} \right)^2 + 2 \frac{\epsilon_s N_D}{eD_s^2} (E_g - \varphi_n - \varphi_o) \right]^{1/2} \tag{16}$$

Therefore, according to Eq. (14), the $1/C^2$ intercept V_o tends to infinity as δ gets large. This indicates that the behavior of V_o and V_{BO} predicted by Eqs. (14) and (15) is at least qualitatively consistent with the observed behavior.

An exact fit of the V_o and V_{BO} data could probably be made if sufficient experimental data for different known interfacial layer thicknesses were available. Since such an analysis is not germane to the present research and since in any case the interfacial layer thicknesses are not known, this has not been attempted here. However, some representative curves of V_o and V_{BO} vs. δ using likely values for the parameters φ_m, φ_o, D_s, X_s, and ϵ_i, have been computed from Eqs. (14) and (15); these curves are presented in Appendix B.

Alternate Model

It will be shown in this section that the GaP/Pt diodes are well characterized by models based on the metal/interfacial layer/semiconductor structure, if certain assumptions regarding the bias dependence of the surface-state charge are made. The detailed analyses of the various models for a metal/semiconductor surface barrier appear in Appendix B.

It is worth repeating at this point the general features required of a model which correctly describes GaP/Pt diodes. Based on experimental observations in this laboratory and on the published results of a study by Cowley and Heffner,[17] we require the diode model to predict the following behavior:

1. The $1/C^2$ vs. V relation must be linear, with a slope of $2/e\epsilon_s N_D$, where ϵ_s and N_D are the semiconductor permittivity and donor density, respectively, and e is the electronic charge.
2. The voltage-axis intercept V_o of the $1/C^2$ vs. V relation must increase rapidly, with increasing interfacial layer thickness.
3. For thin interfacial layers, V_o must agree closely with the diffusion potential, V_{BO}.
4. For all but the thinnest interfacial layers, the diffusion potential must remain relatively constant, with changes in the thickness of the interfacial layer.

The assumption that changes in surface states charge with bias are given by the expression

$$\Delta Q_{ss} = - eD_s(\Delta - \Delta_o) \quad , \tag{17}$$

which results in expressions for V_{BO} and V_o that satisfy all but the second of the requirements listed above. The assumption is a reasonable one for very thin layers. We may therefore conclude that the proposed model for thin layers is a reasonable one.

For thicker interfacial layers, it has been pointed out the assumption $\Delta Q_{ss} = 0$, while predicting substantially correct behavior for V_o and V_{BO} for very thick layers, is not <u>a priori</u> reasonable. An alternative to this assumption is to write ΔQ_{ss} as

$$\Delta Q_{ss} = - eD_s\lambda(\Delta - \Delta_o) \quad , \tag{18}$$

where λ is restricted to be independent of bias and to lie between zero and unity. Use of Eq. (18) results in an expression which satisfies all of the requirements listed above if λ satisfies

$$\lambda \approx 1.0 \quad \delta < \delta_o$$

$$\lambda \to 0 \quad \delta > \delta_o \quad , \tag{19}$$

where δ is the interfacial layer thickness and δ_o is a constant. The exact functional dependence of λ on δ is not known, but is arbitrarily taken to be

$$\lambda = \frac{1}{1 + \exp(\delta - \delta_o)} \quad . \tag{20}$$

This expression evidently satisfies Eq. (19). For the purposes of illustration, δ_o has been taken to be 10 Å for GaP/metal diodes.

It is interesting to consider the possibility a metal/interfacial layer/semiconductor structure without surface states will correctly describe the behavior of the GaP/Pt diodes. This has been explored in detail in Appendix B, and a convincing argument against this model has been formulated. Figure 12 shows a plot of both V_o and V_{BO} calculated on the basis of this model, and although V_o has the correct qualitative variation with δ, the decrease in V_{BO} shown in the figure is not observed experimentally.

The dependence of V_{BO} on metal and semiconductor parameters, surface-state density, and interfacial layer thickness has been derived in Appendix B. Figure B-9 is a plot of V_{BO} vs. δ for the GaP/Au diode, which is qualitatively similar to the GaP/Pt diode. For comparison, V_o is plotted for the thin layer assumption [Eq. (18)], and it is seen that the agreement between V_o and V_{BO} is indeed close for this model. Referring to Table II, the equations corresponding to these curves are Nos. 1 and 4. This model is evidently not valid for thicker interfacial layers, since it violates the second of our list of requirements.

For the assumption $\Delta Q_{ss} = 0$, the uppermost curve of Fig. B-9 is obtained for GaP/Au, corresponding to Eq. No. 2 of Table II, with $\lambda = 0$.

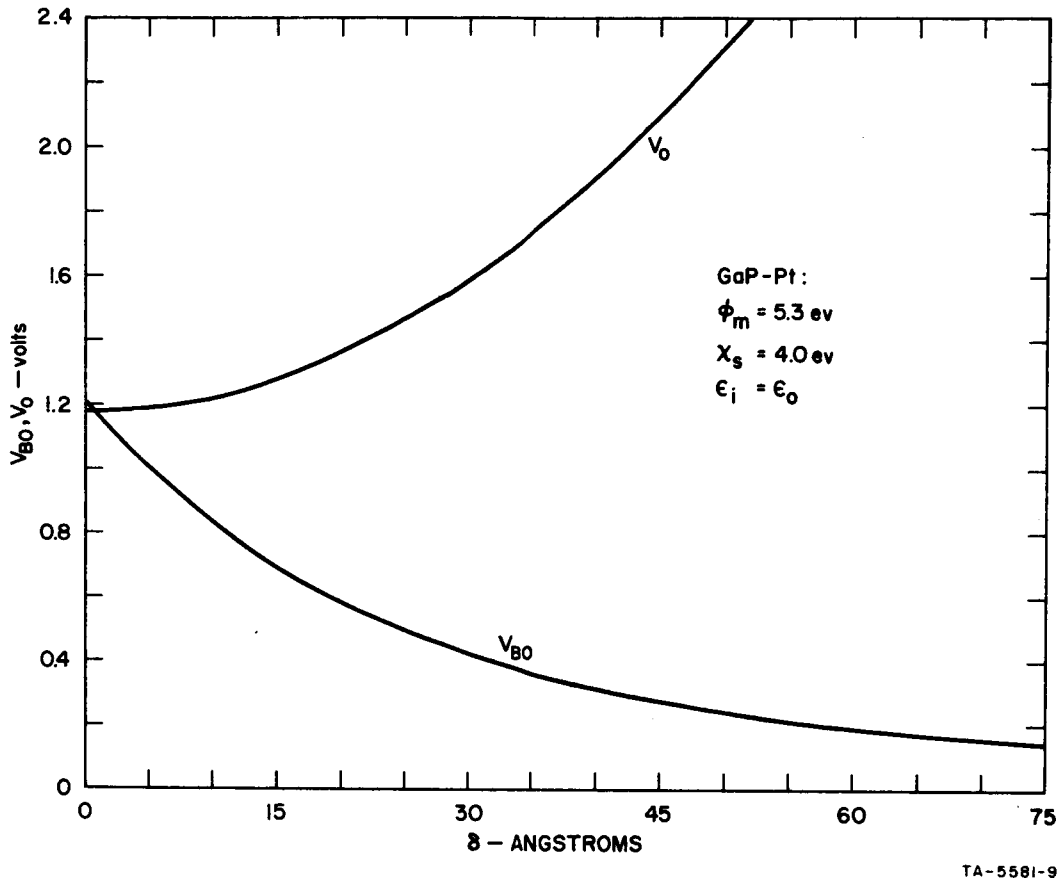

FIG. 12 DIFFUSION POTENTIAL V_{BO} AND INTERCEPT V_o OF $1/C^2$ vs. V PLOT, PLOTTED AS FUNCTIONS OF INTERFACIAL THICKNESS δ

Table II

ASSUMPTIONS REGARDING SURFACE-STATE CHARGE VARIATION WITH BIAS FOR DIFFERENT REGIONS OF LAYER THICKNESS AND THE RESULTING EQUATIONS FOR V_o

Interfacial Layer	Assumed ΔQ_{ss} Variation	Resulting Equation for V_o
1. Thin ($\delta < 10\text{Å}$)	$\Delta Q_{ss} = -eD_s(\Delta - \Delta_o)$	$V_o = [\varphi_{ms} + \alpha(E_g - \varphi_o - \varphi_n)]/(1+\alpha) + \frac{1}{4}V_1/(1+\alpha)^2 - V_2$ $V_o = V_{BO} + V_1^{1/2}(V_{BO} - V_2)^{1/2}/(1+\alpha) + \frac{1}{4}V_1/(1+\alpha)^2 - V_2$
2. Intermediate ($10\text{Å} < \delta < ?$)	$\Delta Q_{ss} = -eD_s\lambda(\Delta - \Delta_o)$ $0 \le \lambda \le 1.0$	$V_o = V_{BO} + V_1^{1/2}(V_{BO} - V_2)^{1/2}/(1+\alpha\lambda) + \frac{1}{4}V_1/(1+\alpha\lambda)^2 - V_2$
3. Thick ($\delta > ?$)	$\Delta Q_{ss} = eD_s(V + \Delta_o - \Delta)$	$V_o = (1+\alpha)V_{BO} + V_1^{1/2}(V_{BO} - V_2)^{1/2} + \frac{1}{4}V_1/(1+\alpha) - (1+\alpha)V_2$
4. Variation of V_{BO} with δ: $V_{BO} = [\varphi_{ms} + \alpha(E_g - \varphi_o - \varphi_n)]/(1+\alpha) + V_1/2(1+\alpha)^2$ $- \left[(1+\alpha)V_1(\varphi_{ms} + \alpha\{E_g - \varphi_o - \varphi_n\}) + \frac{1}{4}V_1^2\right]^{1/2}/(1+\alpha)^2$		
5. Definition of Symbols:* $\alpha = +eD_s\frac{\delta}{\epsilon_i}$; $V_1 = 2e\epsilon_s N_D\frac{\delta^2}{\epsilon_i^2}$; $\varphi_{ms} = \varphi_m - (\chi_s + \varphi_n)$		

*See Figs. B-6 and B-7 of Appendix B for further definitions.

The qualitative behavior of V_o is seen to be correct for thicker interfacial layers, but the behavior for $\delta \geq 10$ Å is not consistent with experiment.

Figure 13 shows the variation of V_o with δ for GaP/Pt, for the assumption of Table II Eq. (2), and with the functional dependence of

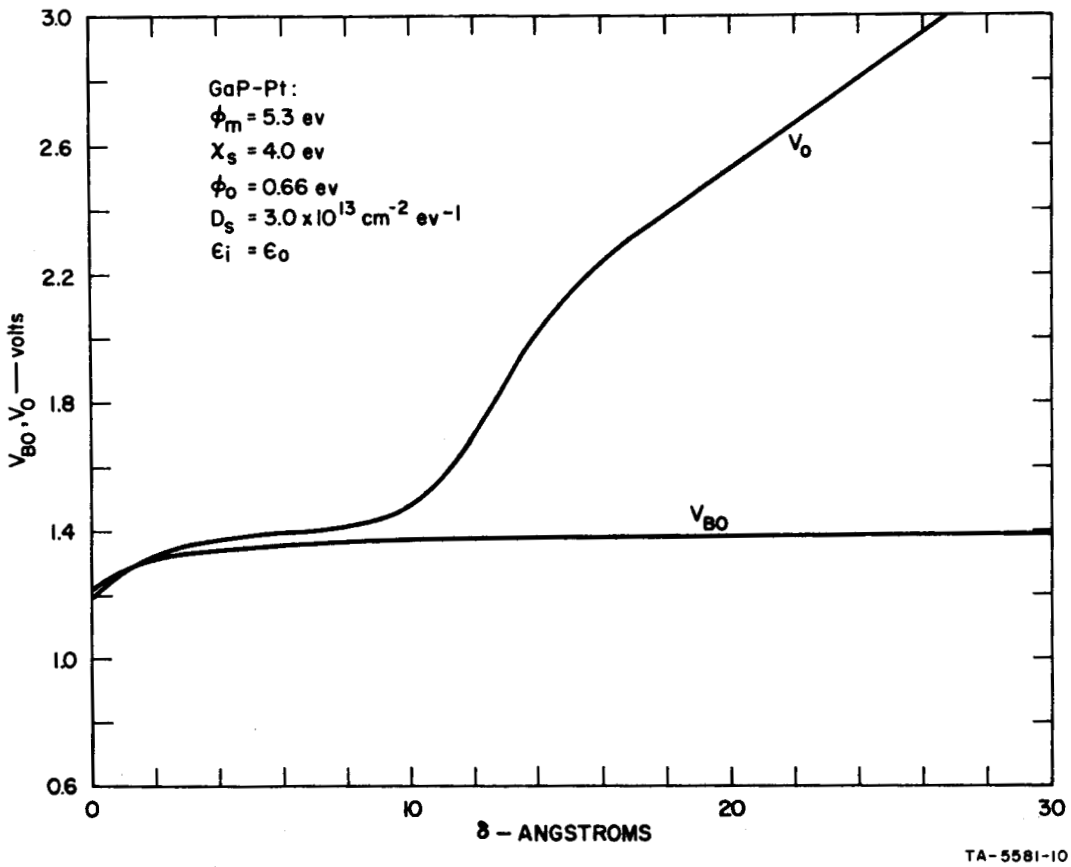

FIG. 13 DIFFUSION POTENTIAL AND $1/C^2$ vs. V INTERCEPT FOR A GaP/Pt DIODE — ELECTRON AFFINITY x_s = 4.0 eV

λ on δ given by Eq. (4). The behavior of V_o depicted here is now entirely consistent with the observed experimental results. The detailed arguments in support of the metal/interfacial layer/semiconductor system with $\Delta Q_{ss} = - eD_s\lambda(\Delta - \Delta_o)$ are presented in Appendix B.

Figure 14 shows the dependence of V_{BO} on δ for a number of different φ_{ms} values, corresponding to Pt, Au, Cu, Ag, Al, and Mg. The behavior

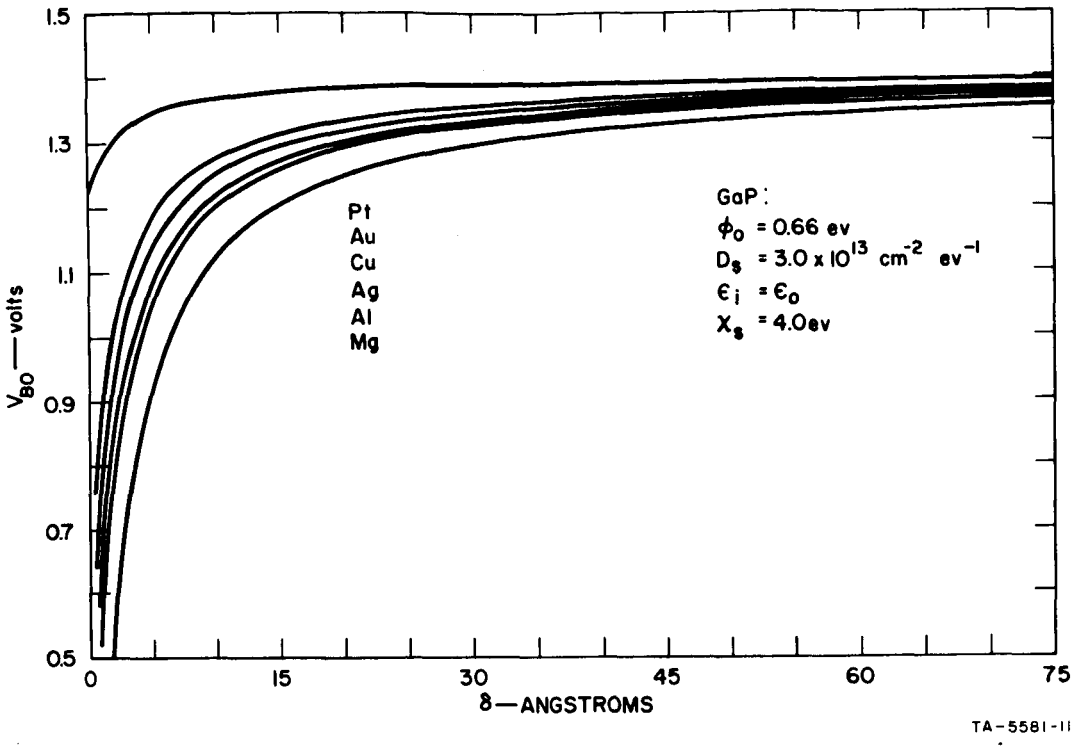

FIG. 14 V_{BO} vs. δ FOR VARIOUS METALS ON GaP — ELECTRON AFFINITY x_s = 4.0 eV

of these curves is interesting in that, for a given metal, there is a considerably large range of δ for which V_{BO} is relatively constant, consistent with the observed behavior of GaP/Pt diodes. Similar behavior has, in fact, been observed by Cowley and Heffner[17] for GaP/Au diodes, and by Cowley (Appendix B) for GaP/Ag, Cu, Al, and Mg diodes.

If, for a given value of δ, the values of V_{BO} are taken from Fig. 16 for each metal, these values can be plotted against the values of φ_m (work function) corresponding to each metal. Figure 15 shows such a plot, with the measured values of V_{BO} shown for comparison (A. M. Cowley and S. M. Sze, Ref. 18). The theoretical curve is indeed linear, as shown by Cowley and Sze, and the best fit to the measured data was found for δ = 7 Å.

Figures 16 and 17 give the same information as Figs. 13 and 14, respectively, but with a different value of electron affinity χ_s chosen for GaP.

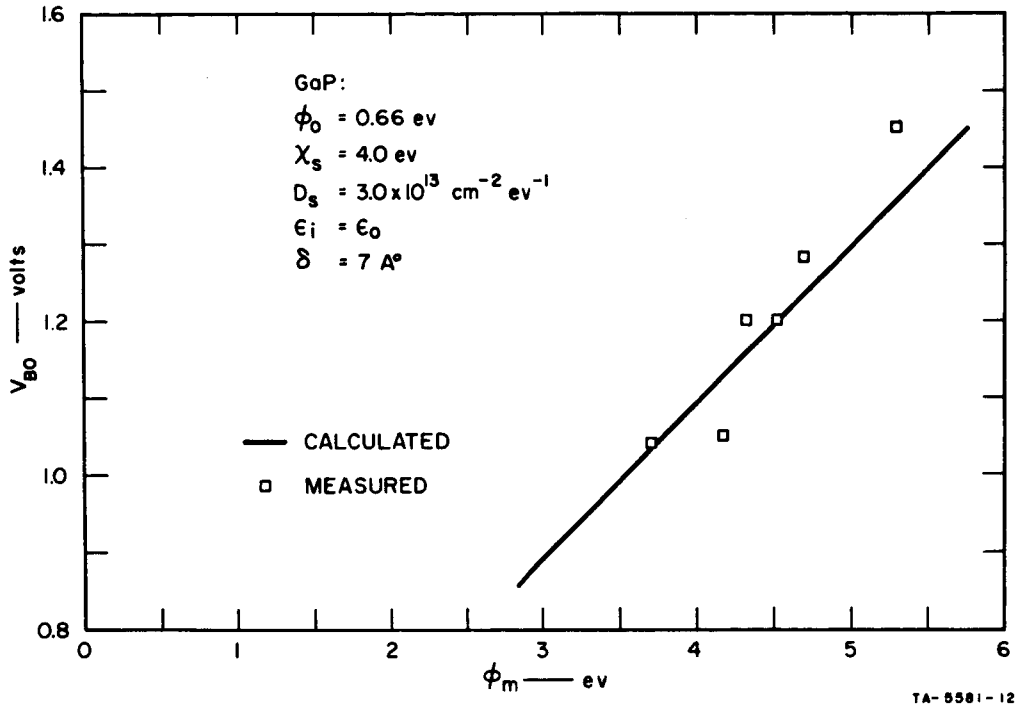

FIG. 15 V_{BO} vs. ϕ_m FOR GaP, ACCORDING TO THEORETICAL EXPRESSION (Eq. 4 of Table II)

3. An Alternative Approach

Scheer and van Laar[19] have recently shown that an essentially zero value of electron affinity can be obtained by depositing a small amount of Cs onto the surface of a p-type GaAs crystal. For a heavily-doped crystal the band bending at the surface occurs over a very short distance. Electrons near the bottom of the conduction band as a result can have a high probability of traversing the band-bending region without scattering, and thus can enter the vacuum. In the experiments of Scheer and van Laar[19], the conduction-band electrons were created by photon absorption. Quantum efficiencies in terms of photo-emitted electrons per absorbed photon of greater than 50 percent were achieved.

An alternative and efficient way of establishing a large number of conduction-band electrons in a p-type region is to forward-bias an n-p junction arranged so that the number of electrons injected from the n-region into the p-region greatly exceeds the number of holes injected

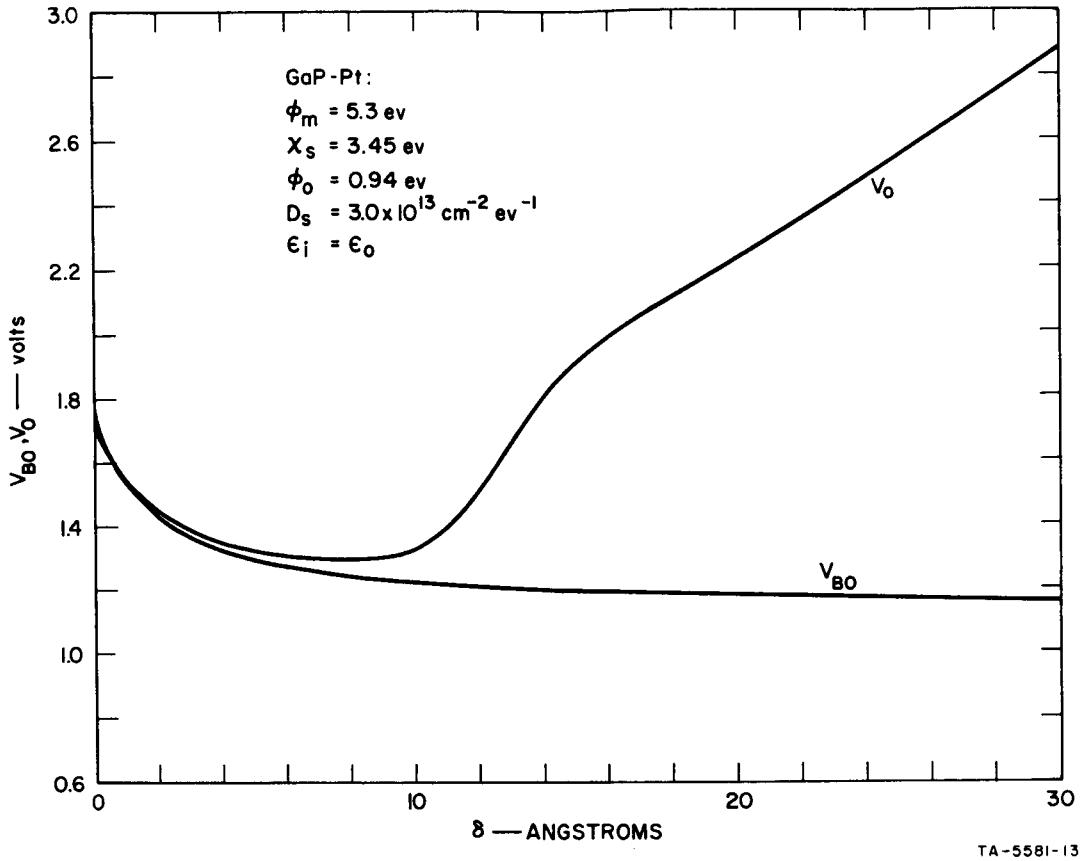

FIG. 16 DIFFUSION POTENTIAL AND $1/C^2$ vs. V INTERCEPT FOR GaP/Pt DIODE — ELECTRON AFFINITY x_s = 3.45 eV

from the p-region into the n-region. (This can be achieved in ways commonly employed for n-p-n transistors.) In effect, such a device is very similar to an n-p-n transistor, except the collector is the vacuum instead of another n-type semiconductor region. Figure 18 shows energy diagrams for the resulting cathode, without and with bias voltages applied.

The n-p Junction or simply Transistor Cathode has a number of potential advantages over the Surface-Barrier Cathode. These can be summarized as follows:

(1) Higher efficiency should result because there are no electrons lost in traversing a metal film.

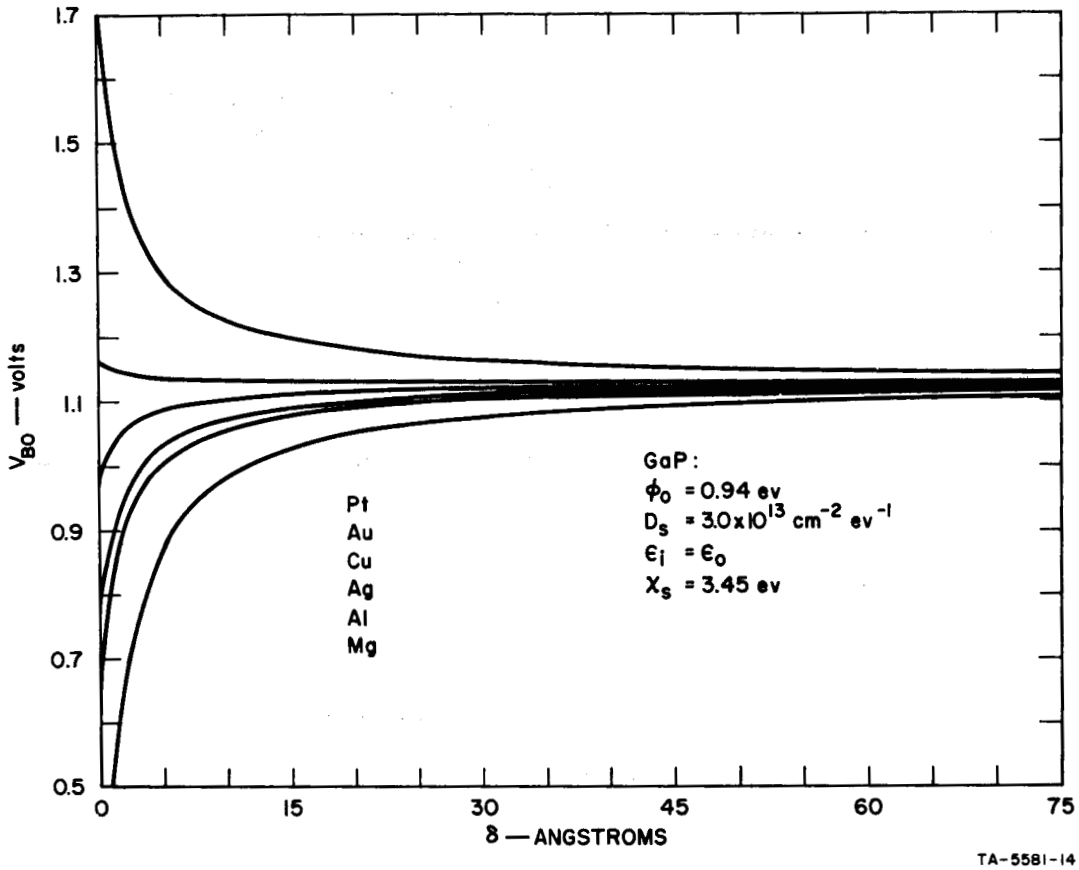

FIG. 17 V_{BO} vs. δ FOR VARIOUS METALS ON GaP — ELECTRON AFFINITY x_s = 3.45 eV

(2) Higher current densities into the vacuum should be achievable because there is no thin metal film to burn out at high current levels.

(3) Calculations indicate a lower sheet resistance can be obtained with one micron of degenerate p-type GaAs than with 100 Å of metal. This obviates the necessity for a grid overlay. (The grid lowers the efficiency.)

(4) The p-n device should be easier to fabricate because the metal film is eliminated as well

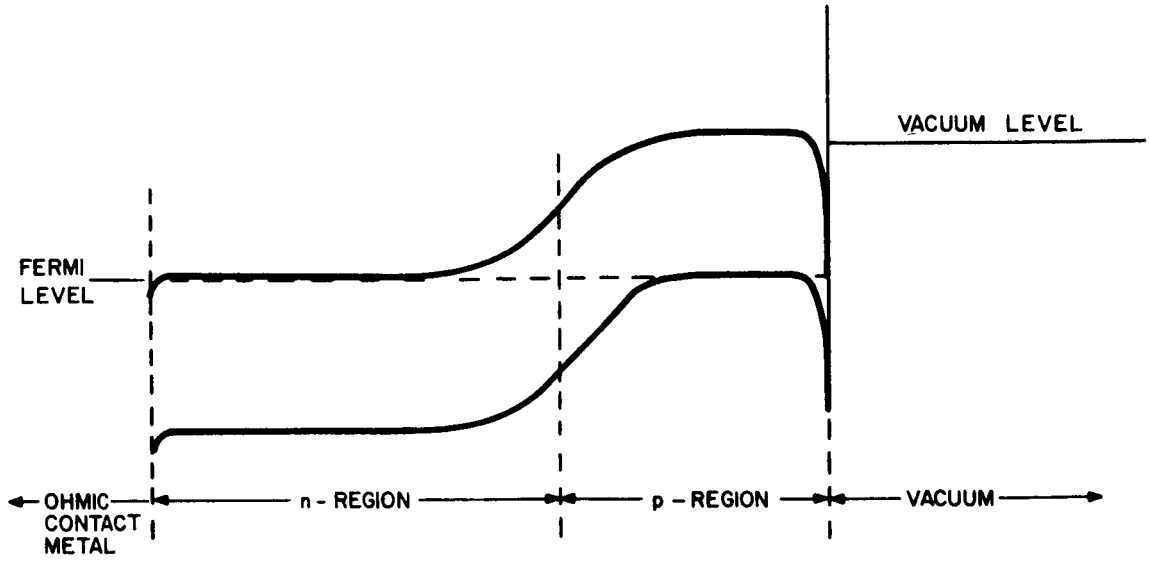

(a) WITH NO BIAS VOLTAGE APPLIED.

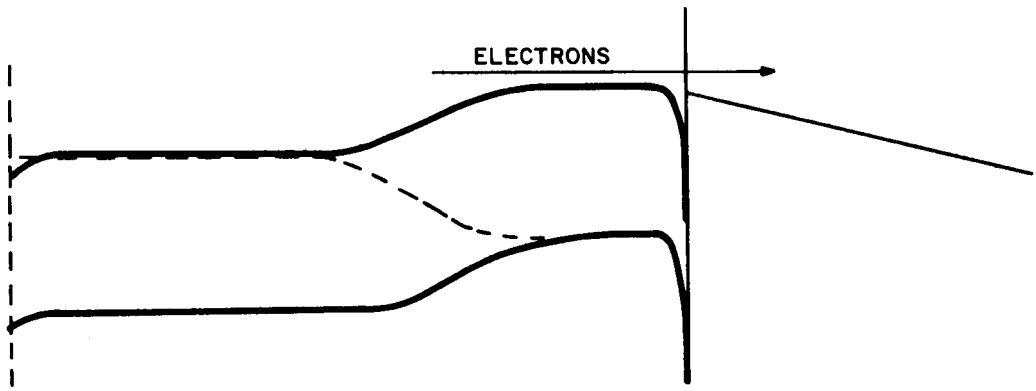

(b) WITH BIAS VOLTAGE APPLIED.

FIG. 18 ENERGY DIAGRAMS FOR n-p FUNCTION CATHODE

as the grid. It also should be easier to make an ohmic contact to the p-type GaAs, rather than to make good contact to a thin metal film, even with a grid.

A wafer of heavily-doped, p-type GaAs has been ordered so initial evaluation studies can be conducted relevant to this approach. We hope in particular a zero or slightly negative electron affinity can be achieved using BaO instead of Cs.

D. LIFE TESTS

1. GaP/Pt Diode

The current-voltage characteristic of a GaP/evaporated Pt diode on dynamic life test was included in the First Quarterly Report[1] on this program. This diode has now been operating on a laboratory bench in the clean room for more than 3500 hours with no apparent change in its characteristics.

2. Ag/BaO Phototube

The response of a glass Ag/BaO phototube was measured at frequent intervals. The average value of the photoelectric work function from these measurements is 1.42 eV. The last measurement after 8900 hours of shelf life was 1.48 eV. There are areas on the surface of the cathode that are more active than others, and by focusing the light on these areas, values as low as 1.35 eV have been obtained.

III CONCLUSIONS AND SUMMARY

Gallium phosphide/tungsten diodes prepared in an oil-free vacuum system produce a surface barrier height of 1.42 eV ± ~.03 eV. There is little or no evidence of a contaminating interfacial layer, as was the case for diodes prepared in an oil-diffusion-pumped vacuum system. There is evidence, however, the barrier is not uniform over the entire surface area. This non-uniformity could reduce efficiency of the cathode at low bias levers. It should not, however, impair the performance appreciably at high bias levels.

The work function of evaporated barium-oxide (BaO) on evaporated tungsten (W) is 1.45 eV ± ~ 0.06 eV. This value is reached after an evaporation time of about 30 minutes with a platinum (Pt) boat temperature of 1100°C. For times shorter than this the BaO film is believed to be discontinuous. For thicker films of BaO, the work function increases slightly, and there is evidence of electron scattering in the BaO film commencing.

A vacuum of better than 10^{-9} Torr is required to maintain a low work function with evaporated BaO films. The partial pressure of water vapor is probably the most important factor in maintaining the low work function. It is believed that a better bake-out is needed for the vacuum system than has been possible so far. Steps are being taken to secure a better bake-out.

A study of the evaporation of BaO indicates little or no free barium should be liberated provided a non-reacting boat material such as Pt is used. We have therefore increased our evaporation rate to about one monolayer per minute by increasing the source temperature to 1100°C.

A study of capacitance vs. voltage and hot-electron data was taken on GaP/metal, surface-barrier diodes. This indicates the semiconductor/interfacial layer/metal model can correctly describe the observed behavior with different interfacial layer thicknesses if certain reasonable assumptions are made regarding the bias dependence of charge contained in surface states.

An alternative cathode approach has been suggested that appears to offer several important advantages over the surface-barrier cathode. In particular, much higher emission efficiencies should be achievable with this alternative approach.

Further life testing indicates the surface-barrier cathode should have an indefinitely long and stable life.

IV PROGRAM FOR NEXT INTERVAL

1) Confirm height of GaP/W barrier using $1/C^2$ vs. V and photoelectric measurements.

2) Determine effect of evaporating a partial monolayer of Ba onto the BaO after optimum activation of evaporated W film.

3) Determine relationship between W film thickness and deposition parameters.

4) Secure and evaluate heavily-doped p-type GaAs for application to transistor-cathode concept.

5) Continue life testing of BaO phototubes and GaP diode structures.

APPENDIX A

EVAPORATION OF BaO

APPENDIX A

EVAPORATION OF BARIUM OXIDE

1. Species in Vapor

Several references [20,21,22] state the major species formed when barium oxide (BaO) is evaporated is gas (better than 95 percent). That is, the decomposition to Ba (gas) and 1/2 O_2 (gas) is negligible. It is presumed this occurs under neutral or oxidizing conditions.

2. Vapor Pressure of BaO

The literature before 1960 has been analyzed by Ackerman and Thorn[20]. A vapor pressure curve derived from this analysis is shown in Fig. A-1 (upper curve). This is presumably the equilibrium pressure of BaO gas over the solid. Nikonov and Otmakhova[21] have measured the rate of evaporation of BaO from a surface. (Fig. A-2).

When the evaporation rates given in Ref. 21 are recalculated as effective vapor pressures, they give the lower curve shown in Fig. A-1. These rates are about three orders of magnitude lower than the equilibrium values. This may indicate that one of the two sets of experiments is wrong, or that there is a kinetic barrier to the BaO evaporation.

3. Evaporation of Substrate Oxides

The reaction of BaO with a substrate metal (i.e., the metal heater used to evaporate BaO) to form Ba and substrate (volatile) oxide can be important. The possible effects of such reaction are that Ba and the oxide of the substrate can evaporate and be incorporated in the BaO evaporation. The Ba might lower the work function of the oxide, but the higher work function of the substrate oxide would predominate.

To show that a reaction of BaO with the substrate is possible, consider the reaction

$$BaO(s) + 1/3\ W(s) = Ba(g) + 1/3\ WO_3(g) \quad . \qquad (A\text{-}1)$$

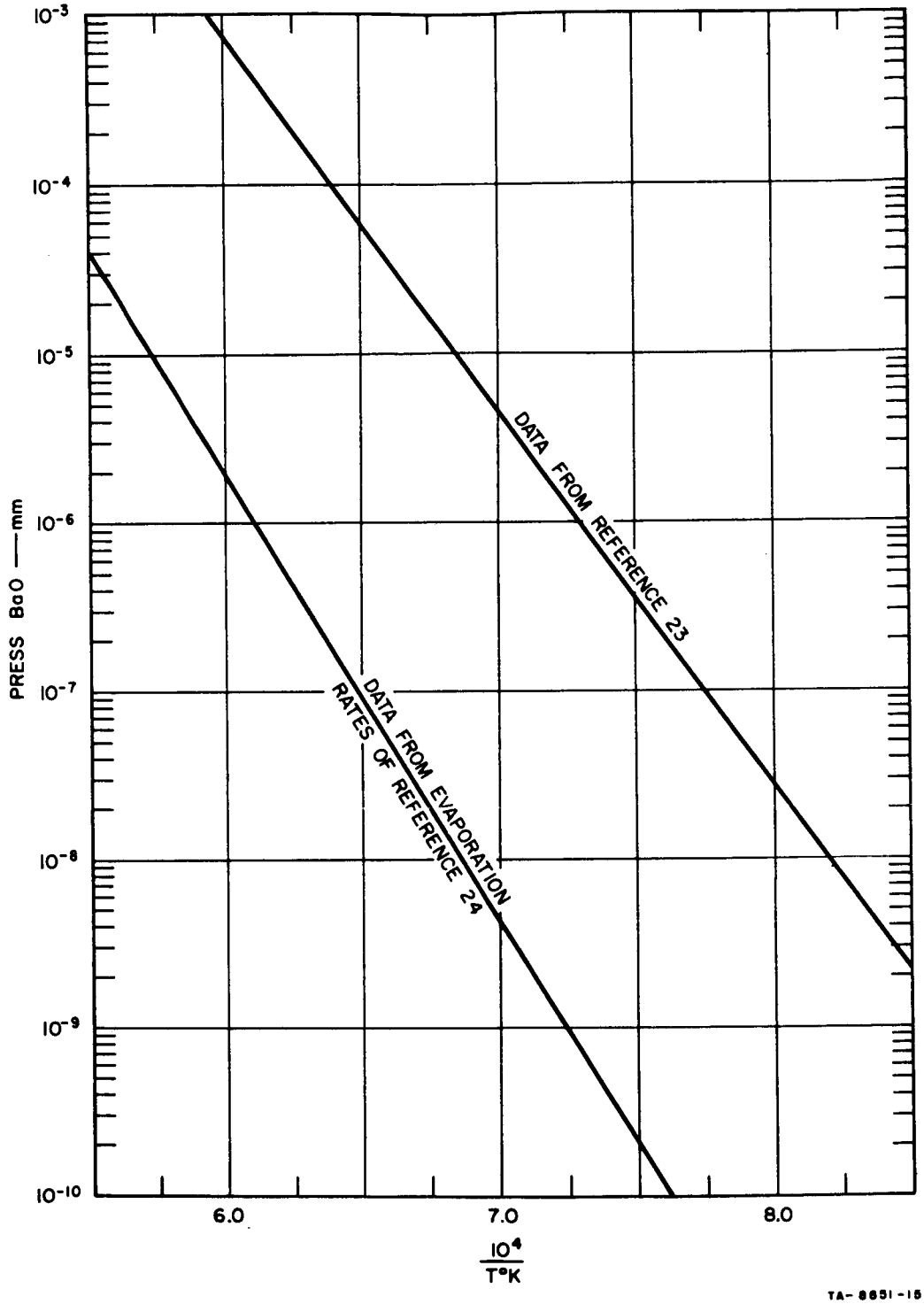

FIG. A-1 EQUILIBRIUM VAPOR PRESSURE OF BaO

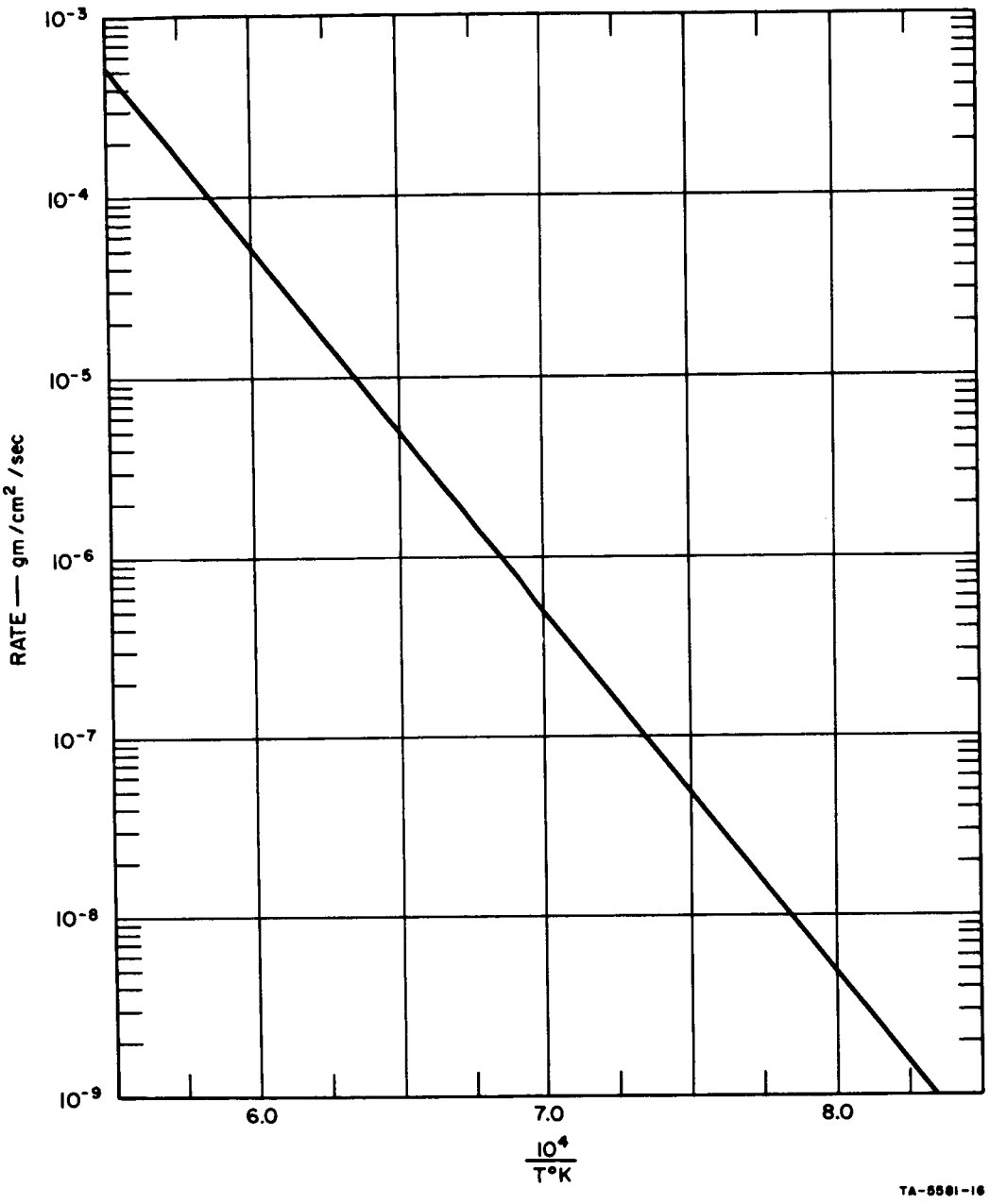

FIG. A-2 RATE OF EVAPORATION OF BaO

From the data of Ref. 20,

$$3/2\ O_2(g) + W(s) = WO_3(g)$$

$$\Delta F^o = -75,000 + 15.54T$$

$$1/2\ O_2(g) + Ba(s) = BaO(g)$$

$$\Delta F^o = -33,400 - 9.68T$$

$$Ba(s) = Ba(g) \quad \log p = \frac{9718}{T} + 4.93$$

$$(\Delta F^o = 44,500 - 22.6T)$$

$$BaO(s) = BaO(g) \quad \log p = 7.11 - \frac{21,900}{T}$$

$$(\Delta F^o = 100,000 - 32.5T) \quad . \qquad \text{(A-2)}$$

One calculates for the reaction of interest,

$$\Delta F^o = 152,000 - 40.24T \text{ (cal/mole)}$$

or, since

$$\Delta F^o = -RT\ \ell n\ K_p,$$

$$\log K_p = 8.8 - \frac{33,400}{T}$$

where

$$K_p = p_{Ba}(atm) p_{WO_3}^{1/3}(atm) \quad . \qquad \text{(A-3)}$$

In Fig. A-3, K_p is plotted for this reaction.

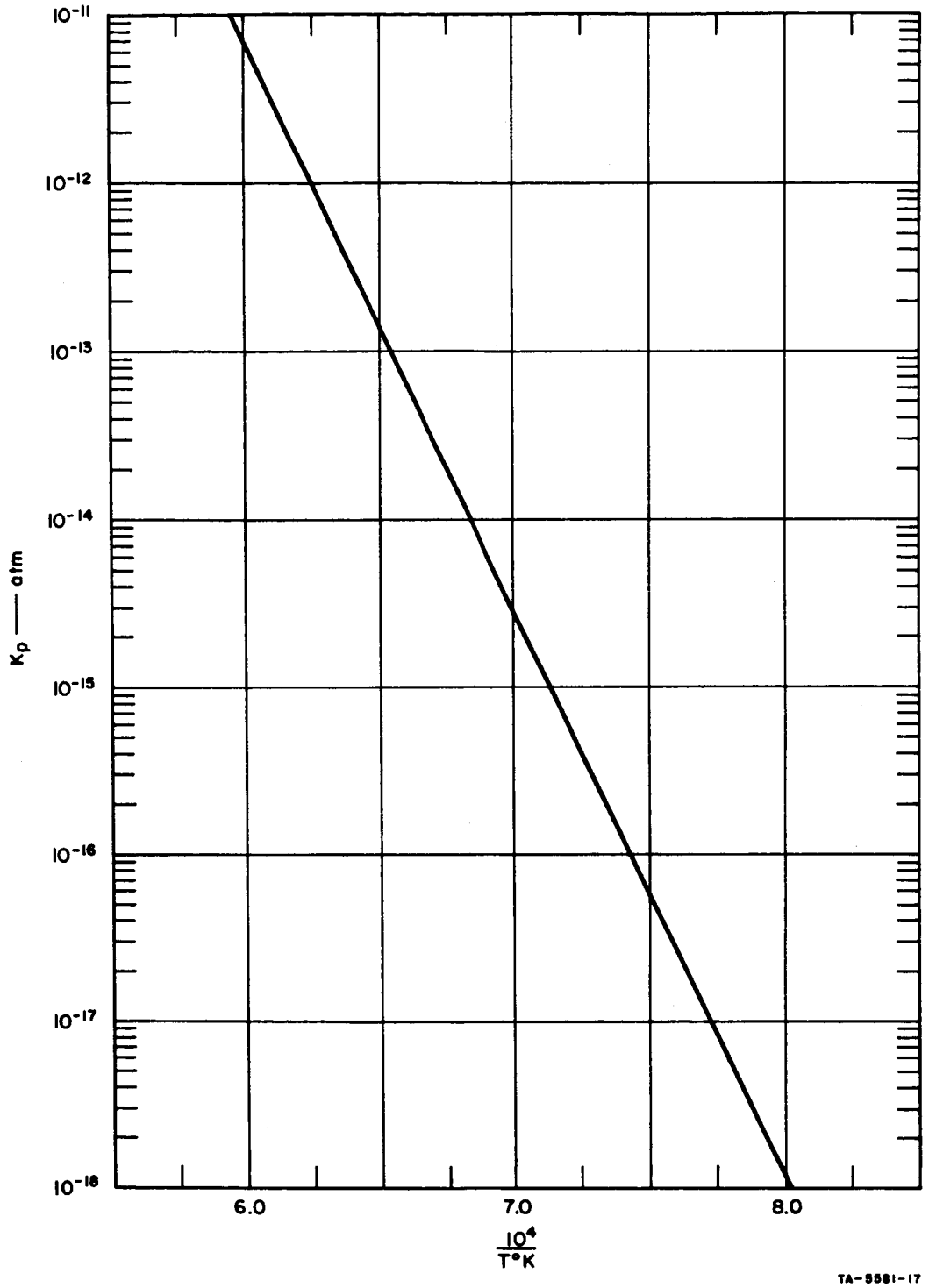

FIG. A-3 EQUILIBRIUM CONSTANT FOR REACTION: BaO(s) + 1/3 W(s) = 1/3 WO_3(g) + Ba(g) $K_p = p_{Ba} \cdot p_{WO_3}^{1/3}$

As a sample calculation at 1600°K, one finds K_p is 10^{-12}; that is $p_{Ba} \cdot p_{WO_3}^{1/3} = 10^{-12}$. If one assumes the $p_{Ba} \approx p_{WO_3}$, then p_{Ba} (or p_{WO_3}) becomes 10^{-9} atm or $\sim 10^{-6}$ mm. At the same temperature the vapor pressure of BaO is 10^{-4} mm (Fig. A-1) so that the equilibrium calculations indicate a percent or so of impurity from this reaction.

These estimates are based on equilibrium considerations, and we have seen that the rate of evaporation of BaO (lower curve of Fig. A-1) is smaller than the equilibrium expected value (upper curve of Fig. A-1); therefore, the fraction of WO_3 and Ba (compared to BaO) may be substantially greater than the 1 percent estimated from equilibrium.

Inghram and Drowart[23] reviewed mass spectrometer observations of the evaporation of BaO from various supports or containers. They give the following information:

Container or Support	Gaseous Molecules Observed (in order of importance)
Mo filament	BaO, Ba, $BaMoO_4$
W filament	BaO, Ba, $BaWO_4$, WO_2
Ta filament	Ba, BaO, Ba_2, TaO_4, TaO, TaO_2
Pt filament	BaO, Ba_2O_2

Thus, the reaction with refractory metal supports can be appreciable, but the effect with a Pt support appears to be reduced.

APPENDIX B

DEPLETION CAPACITANCE AND DIFFUSION POTENTIAL OF GALLIUM PHOSPHIDE SURFACE BARRIER DIODES

APPENDIX B

DEPLETION CAPACITANCE AND DIFFUSION POTENTIAL OF GALLIUM PHOSPHIDE SURFACE BARRIER DIODES

1. Introduction

Two common methods for determining the barrier height φ_{Bn} and diffusion potential V_{BO} of a metal-semiconductor surface barrier diode are the measurement of the threshold V_{ph} for the photoexcitation of carriers over the barrier and the measurement of the depletion capacitance as a function of bias voltage.[14,17,24-28] In the second method the diffusion potential is obtained as the voltage-axis intercept V_o of a plot of the reciprocal square of the depletion capacitance vs. bias voltage ($1/C^2$ vs. V).

For moderately heavily doped semiconductors, the diffusion potential and barrier height are approximately equal. In the last few years, however, several workers[25,28] have reported values of V_o which were considerably larger than the photothreshold V_{ph} for n-type GaP/Au diodes.

It has been recognized[14,17] that this effect is related to the presence of an interfacial layer between the metal and semiconductor, and a model which includes the interfacial layer has been analyzed by Goodman,[14] who has derived an expression which shows that V_o is always larger than V_{BO} when an interfacial layer is present. Goodman assumes that the charge in semiconductor surface states, if any, is independent of applied bias; a similar assumption has been made in the work of Archer and Atalla[24] on silicon. The dependence of V_{BO} on the interfacial layer parameters is not specified in the analyses of either Goodman or Archer and Atalla.

An attempt is made herein to provide an explanation for the behavior of V_o and V_{ph} for n-type GaP-metal diodes with different interfacial layer thicknesses. For this purpose, the model treated by Goodman is modified in two respects:

a. The exact mechanism for the dependence of the diffusion potential on interfacial layer thickness and surface states is specified;

b. the effect of bias-dependent surface states is considered according to several simple models.

Measurements of V_o and V_{ph} for n-type GaP-metal diodes are described in Sec. 2 of this appendix; a brief description of the diode fabrication is also given. Some of the experimental results presented here have been summarized in other publications.[17,18] Briefly stated, the observations of the behavior of $1/C^2$ vs. V data and the photothreshold V_{ph} for a given metal on n-type GaP are as follows:

a. The $1/C^2$ vs. V data for reverse and small forward bias always lie on a straight line whose intercept, V_o, on the V axis may be between 1 and several volts; in general, higher values of V_o are correlated with thicker interfacial layers.

b. The photothreshold V_{ph} is constant within a few tens of millivolts, independent of the interfacial film thickness δ.

c. The slope of the $1/C^2$ plot is relatively constant, independent of interfacial layer thickness, and for most diodes the donor density calculated from the $1/C^2$ vs. V slope using the usual formula agrees within a factor of 2 with the value determined from the resistivity. No correlation was observed between the slope of the $1/C^2$ vs. V curve and the presence or absence of an interfacial layer.

A model which correctly describes the behavior of the n-type GaP-metal system with variation of the interfacial film thickness δ must therefore show V_{BO} relatively constant with δ, and V_o increasing with δ. The $1/C^2$ vs. V relation derived on the basis of the model must be linear, with a slope that is independent of δ.

It is shown in Sec. 3a of this appendix that the dependence of V_{BO} and V_o on δ, derived on the basis of a simple metal-interfacial layer-semiconductor (MOS) model without "surface states," is completely at variance with the general observations regarding experimental data given above. Sections 3b, 3c, and 3d are accordingly devoted to the analysis of the MOS model with surface states, where the surface states are assumed to be uniformly distributed over a range of energies in the forbidden gap.[29] Section 3b applies to very thin interfacial films, where

the Fermi level at the semiconductor surface is expected to remain "pinned" to the Fermi level in the metal during the application of a bias.[24] In Sec. 3c the assumption is made that the charge in surface states, Q_{ss}, does not change with bias; Sec. 3d treats a model which provides for a transition from the model of 3b to the model of 3c as δ increases.

It is shown that the model of Sec. 3b predicts a variation of V_{BO} and V_o with δ which is consistent with the experimental behavior of the diodes with the thinnest interfacial films. The model of Sec. 3c, while predicting a rapid increase of V_o with δ and a relatively small change in V_{BO}, as required to explain the data for the thicker interfacial films, predicts a difference in V_{BO} and V_o which is too large for very small δ ($\sim$ 10 Å). The assumption of $\partial Q_{ss}/\partial V = 0$ for this model is a priori unreasonable anyway, and accordingly, the model of Sec. 3d has been designed to provide a more physically reasonable variation of Q_{ss} with V. The variations of V_{BO} and V_o with δ derived on the basis of this model are consistent with experiment.

2. Experiments

a. Substrate Preparation

The diodes described in this study were prepared from single crystal 0.2 Ω-cm n-type GaP grown at Bell Telephone Laboratories, Murray Hill, New Jersey.[30] The crystals were supplied in the form of 1/4-inch diameter × 0.030-inch thick wafers. The flat surfaces of the wafers were perpendicular to the {111} crystallographic direction. The wafers were lapped with No. 3200 carborundum powder and wet-polished to a mirror finish with Linde A abrasive compound. Ohmic contacts were attached by alloying small ($\sim$ 50 mg) pieces of Te-doped (1.0%) silver to the periphery of one side of the wafers. Allowing was done at 800° C in an atmosphere of forming gas (90% N_2, 10% H_2). The ohmic contacts thus obtained had low electrical resistance ($<$ 10 Ω) and good mechanical strength.

Due to a lack of inversion symmetry in the {111} direction, the two sides of a GaP wafer cut perpendicular to the {111} direction must be distinguished; one side is bounded by a (111) plane, containing only

phosphorous atoms, and the other side by a $(\bar{1}\bar{1}\bar{1})$ plane, containing only gallium atoms.[31] Although it is possible, in principle, to determine experimentally the crystal plane corresponding to a given side of the wafer by using X-ray diffraction data, this was not done in the present work. Instead, it was observed for GaP/Al diodes that there was a consistent difference of about 0.1 ev in the barrier height, depending on which side of the wafer was used to form the rectifying contact. Subsequent diodes using other metals were prepared using the crystal face which yielded the lower barrier height with aluminum. The results reported here and in Ref. 18 are thus consistent among themselves, in the sense that the same crystal face was used in all experiments. It is not known, however, whether this face corresponds to the "phosphorous plane" or the "gallium plane."

Prior to evaporation of rectifying contacts, the surface of each crystal was etched in (4:1) aqua regia at 20°C for 60 seconds and quenched in methanol. The ohmic contacts were protected with Apiezon wax during this operation. After removing the Apiezon wax with tricholorethylene and rinsing in acetone, the substrate was placed in a conc. HNO_3 etch for 1 minute, followed by a methanol quench. Except where noted, the substrate was stored in methanol until it was placed, still wet, in the vacuum system.

b. Evaporation of Metallic Contacts

Rectifying contacts were deposited on the surface of the GaP wafers by vacuum evaporation of Pt, Au, Cu, Ag, Al, and Mg from resistance-heated sources. For all metals but Pt, films about 1000 Å thick were deposited. The Pt films were generally somewhat thinner, about 500-600 Å.

The geometry of the rectifying contacts was controlled by 0.005-inch molybdenum masks; large rectangular contacts, 0.10 × 0.20 inch, were provided for photothreshold measurements, while smaller circular contacts, 0.020-inch diameter, were used for capacitance and current vs. voltage measurements.

Two different vacuum stations were used for evaporation of contacts. The first group of devices was prepared in a liquid N_2-trapped oil diffusion-pumped station capable of about 5×10^{-7} torr. No attempt was made here to shutter the evaporation source, although sources were fused and pre-outgassed prior to placing the substrate in the vacuum station. A second group of devices was prepared in a Varian Vac-Ion vacuum station capable of about 10^{-8} torr. In this case the evaporation sources were shuttered, and a stream of evaporating metal was established before the shutter was opened.

c. Measurements

Photoresponse measurements were made by shining monochromatic light from a Leiss single-flint glass-prism monochromator through the substrate onto the large metal contact and measuring the short-circuit photocurrent with an HP 425A microvolt-ammeter. Measurements were made for photon energies between 1.0 and 2.5 eV. Illumination for the monochromator was provided by a tungsten-filament motion-picture projector lamp. The intensity of the monochromator output was calibrated with a Reeder vacuum thermopile having a sensitivity of 8 microvolts per microwatt.

Capacitance measurements were performed with a Boonton Model 75A capacitance bridge, with an oscillator frequency of 1 Mc. Bias for the diodes was supplied internally, and the ac signal across the junction in all cases was less than 15 mV. Bias was measured with a Hewlett-Packard Model 412A dc VTVM.

d. Results

The most detailed investigation of the effects of interfacial layers on V_o and V_{ph} has been made for GaP/Au and GaP/Pt diodes. For the sake of brevity, the presentation and discussion of experimental results will be confined to these cases. All of the results presented here, however, are in qualitative agreement with the results for Al, Mg, Ag, and Cu/GaP diodes. Table B-1 summarizes the photothreshold and $1/C^2$ intercept values obtained for a number of GaP/Au and GaP/Pt diodes.

Table B-1

PHOTOTHRESHOLD AND $1/C^2$ INTERCEPT VALUES

FOR GaP/Au AND GaP/Pt DIODES

Sample No.	Metal	V_o	V_{ph}	$N_D \div 10^{17}$ cm^{-3}	Vacuum
3	Au	1.9	--	3.5	10^{-6} torr; oil diffusion
4	Au	2.2	--	3.0	10^{-6} torr; oil diffusion
5	Au	1.85	1.26	5.3	10^{-6} torr; oil diffusion
6	Pt	7.0	--	1.2	10^{-4} torr; oil diffusion
7	Pt	3.3	--	0.9	10^{-5} torr; oil diffusion
8	Pt	2.1	1.45	6.9	10^{-5} torr; oil diffusion
9*	Au	2.1	1.23	2.7	10^{-6} torr; oil diffusion
10†	Au	1.6	1.26	4.0	10^{-8} torr; Vac-Ion
11†	Au	1.5	--	2.5	10^{-8} torr; Vac-Ion
12	Au	1.35	1.30	3.6	10^{-8} torr; Vac-Ion
13	Au	1.42	1.28	9.8	10^{-8} torr; Vac-Ion
14	Au	1.28	1.26	3.1	10^{-8} torr; Vac-Ion
14	Au	--	1.25§	--	10^{-8} torr; Vac-Ion
14	Pt	1.45Δ	1.26	3.1	10^{-7} torr; Vac-Ion
18	Pt	1.45	1.43	0.8	10^{-7} torr; Vac-Ion
19	Pt	1.55	1.46	0.8	10^{-7} torr; Vac-Ion
20	Pt	1.48	1.44	1.5	10^{-7} torr; Vac-Ion

*Substrate exposed to atmosphere for 60 min. prior to evaporation of Au.

†Substrate exposed to atmosphere for 15 min. prior to evaporation of Au.

§Measurement performed at 77° K.

ΔDiode allowed to stand in atmosphere for 4 weeks prior to measurement.

Figure B-1 is a remarkable example of the fact that the $1/C^2$ vs. V plot for the GaP-metal diodes remains linear for a large range of

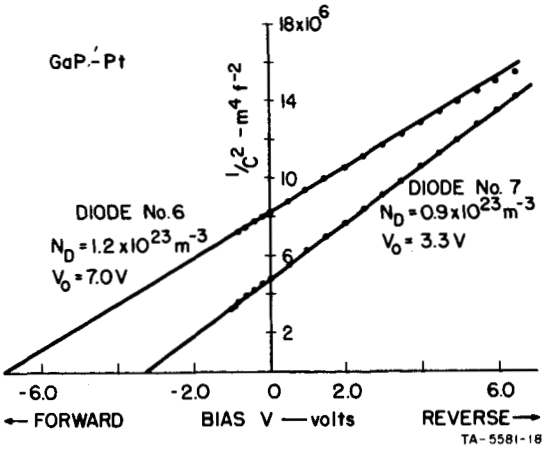

FIG. B-1 $1/C^2$ vs. V PLOTS FOR GaP/Pt DIODES PREPARED IN OIL-DIFFUSION VACUUM SYSTEM
Values of N_D for each curve have been calculated from the usual formula relating N_D to the slope of the $1/C^2$ plot:
$N_D = (2/e\eta_s)/[d(1/C^2)/dV]$.

values for the V-axis intercept V_o. Figure B-2 and B-3 illustrate the same phenomena for GaP/Au diodes. Referring to Table B-1 and Figs. B-4 and B-5, one can observe that while V_o varies over a wide range, the photothreshold for a given metal, in this case Au, remains relatively unchanged. It is also observed that diodes fabricated in the oil-diffusion vacuum system generally exhibit the higher values of V_o, and in fact, all attempts to fabricate diodes in the oil-diffusion system with values of V_o much less than 2.0 V were unsuccessful. Inspection of the data presented in Table B-1 reveals no apparent correlation between the slope and intercept of the $1/C^2$ plots; the spread in values of N_D as determined from the slope of the $1/C^2$ plots is attributed to doping inhomogeneities in the GaP. The average of the values of N_D calculated in this way for all diodes was about 3.6×10^{17} cm^{-3}. A calculation based on the known resistivity, mobility,[33] and donor ionization energy,[34]

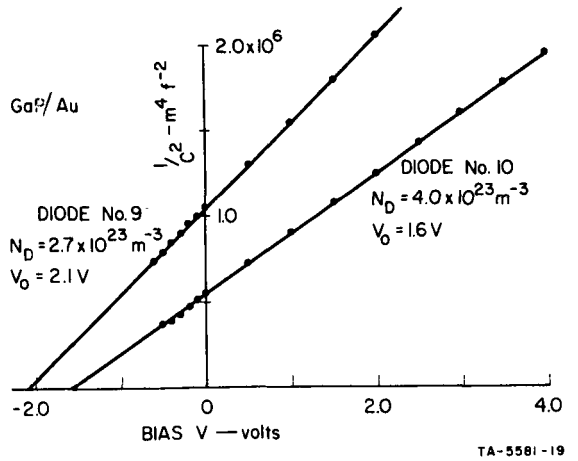

FIG. B-2 $1/C^2$ vs. V PLOTS FOR GaP/Au DIODES PREPARED IN VAC-ION SYSTEM. GaP substrate exposed to air before deposition of Au.

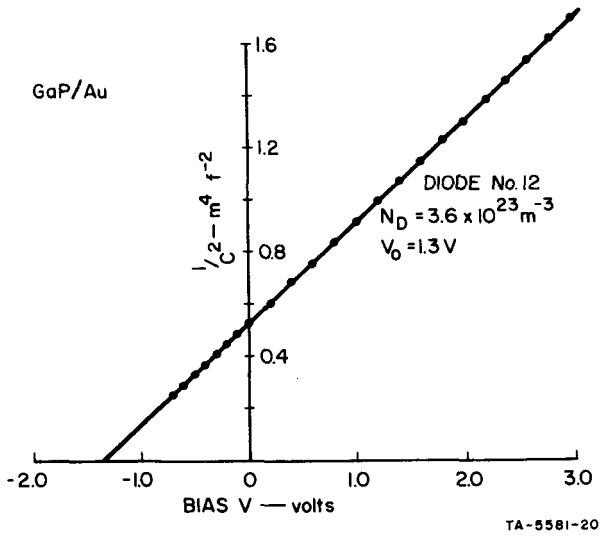

FIG. B-3 $1/C^2$ vs. V PLOT FOR GaP/Au DIODE PREPARED IN VAC-ION SYSTEM. Substrate etched and protected according to procedures described in Sec. II, Appendix B.

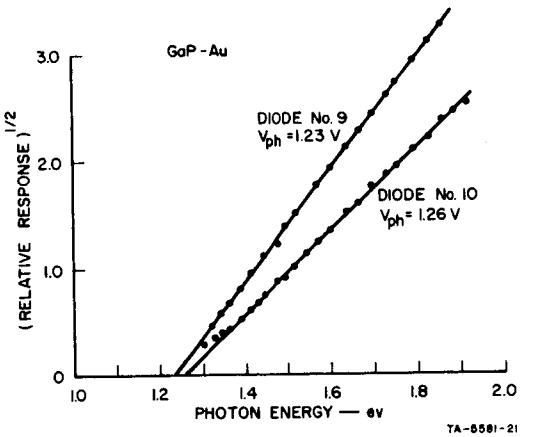

FIG. B-4 PHOTOTHRESHOLD DETERMINATION FOR GaP/Au DIODES WHOSE $1/C^2$ vs. V PLOTS APPEAR IN FIG. B-2

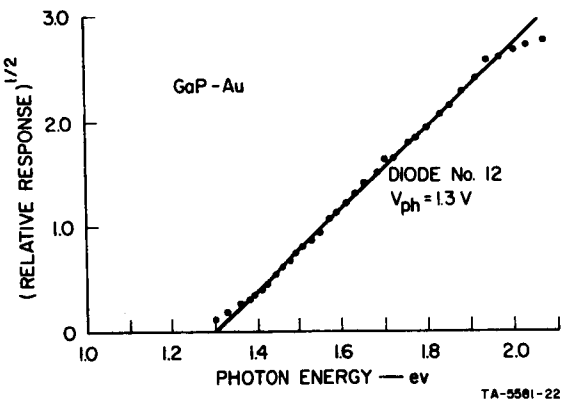

FIG. B-5 DETERMINATION OF PHOTOTHRESHOLD FOR GaP/Au DIODE OF FIG. B-3

and on the estimated density of states effective mass of GaP,[35] indicates that $N_D \cong 5.0 \times 10^{17}$ cm^{-3}. In view of the uncertainties in resistivity and effective mass and the spread in slopes of the $1/C^2$ plots, this agreement is regarded as satisfactory.

Diodes of GaP/Au and GaP/Pt prepared in the Vac-Ion station using etched and carefully protected substrates,[17] as described in Sec. 2a of this appendix, gave values of V_o and V_{ph} that were generally in good agreement (e.g., samples 12, 13, 14, 18, 19, 20, Table B-1; see also Figs. B-3 and B-5). The I-V characteristics of the GaP/Au diodes prepared in this manner obeyed the relation $J = J_o \exp(qV/nkT)$ amps/cm^2 in the forward direction, with n close to unity, usually about 1.1. Calculations using the extrapolated value of J_o yielded values for V_{BO} which agreed within less than 0.1 V with the capacitance and photothreshold values. The GaP/Pt diodes had values of n which were usually greater than 1.5, precluding the use of the I-V characteristics in calculating V_{BO}.

The general behavior of the capacitance data for the GaP/metal diodes leads to the conclusion that larger values of V_o are correlated with thicker interfacial layers. This statement is based on the following reasoning: The highest values of V_o are obtained for diodes prepared in the oil-diffusion system, where back-streaming diffusion pump oil is expected to form a film on the GaP substrate before evaporation of the metallic contact. At a vacuum of 10^{-6} torr, many layers of oil molecules can accumulate in a few seconds, depending on the sticking coefficient of the molecules. Fabrication of diodes in the Vac-Ion station, using identical substrate preparation and protection, produced the lowest values of V_o. The only difference in the two cases seems to be the much higher probability for the formation of an interfacial layer for diodes prepared in the oil-diffusion system. An intermediate case, where substrates were exposed to air prior to being placed in the Vac-Ion station, produced intermediate values of V_o, the interfacial film in this case presumably arising from a chemical reaction of the GaP surface with one of the constituents of the atmosphere. The thinnest interfacial layers are evidently obtained when the GaP substrates are etched and protected in methanol before being placed in the Vac-Ion station.

3. Theory

In this section an attempt is made to assign to the GaP/metal junction a model which correctly predicts the experimental results described in Sec. 2c. Since a model with an interfacial layer but no surface states does appear to be at least partially consistent with the observed behavior of the GaP/metal diodes, particularly the variation of V_o with interfacial layer thickness, it is worthwhile to investigate this model in some detail, in order to show that it is in fact not the correct model. Subsequent models treated in this section all involve the assumption of a uniform density of localized electronic states at the semiconductor surface.

a. Metal-Interfacial Layer-Semiconductor (MOS) Contact without Surface States.

Figure B-6 shows the energy vs. distance diagram for a metal-n-type semiconductor contact with an insulating interfacial layer. In terms of the energies defined in this figure, we may write

$$\varphi_{ms} = V_{BO} + \Delta_o \quad , \tag{B-1}$$

where φ_{ms} is defined by the relation

$$\varphi_{ms} = \varphi_m - (\chi_s + \varphi_n) \quad . \tag{B-2}$$

Using Gauss's law to relate the space charge Q_{sc} in the semiconductor to the potential Δ_o across the interfacial layer, we obtain

$$\Delta_o = \frac{\delta}{\epsilon_i} \left[2e\epsilon_s N_D \left(V_{BO} - V_2 \right) \right]^{1/2} \quad , \tag{B-3}$$

where δ and ϵ_i are thickness and dielectric constant of the insulating layer, respectively; N_D is the donor density in the semiconductor; e the electronic charge; and ϵ_s the semiconductor dielectric constant. The reserve layer term V_2 is a small correction which arises from the presence of mobile carriers in the edge of the depletion region and is derived for the general case of incomplete donor ionization in Appendix C.

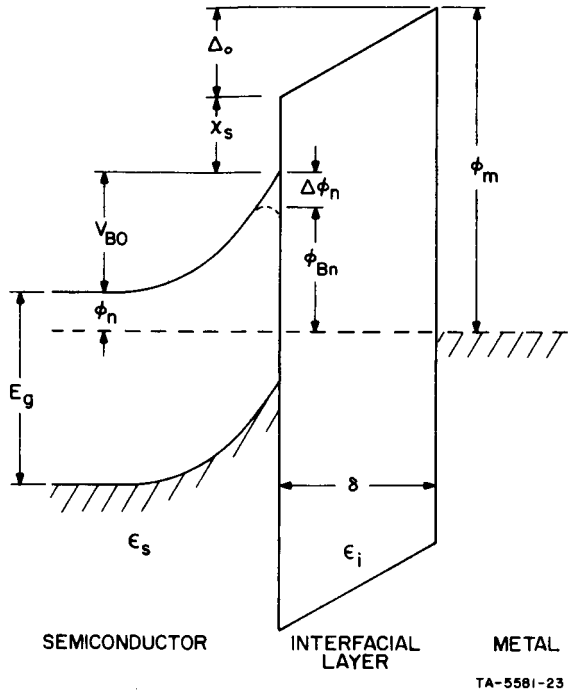

FIG. B-6 BAND DIAGRAM FOR METAL n-TYPE SEMICONDUCTOR CONTACT WITH AN INTERFACIAL LAYER (MOS CONTACT)
ϕ_m = metal work function; Δ_o = potential across interfacial layer; χ_s = semiconductor electron affinity; V_{BO} = diffusion potential in semiconductor; ϕ_n = depth of Fermi level below conduction band in semiconductor; E_g = semiconductor band gap; ϕ_{Bn} = barrier height; $\Delta\phi_n$ = image force lowering; δ = interfacial layer thickness; ϵ_s = permittivity of semiconductor; ϵ_i = permittivity of interfacial layer.

The writing of Eq. (B-3) can be simplified by defining

$$V_1 = 2e\epsilon_s N_D \delta^2/\epsilon_i^2 \quad , \tag{B-4}$$

whereupon Eq. (B-3) becomes

$$\Delta_o = V_1^{1/2}\left(V_{BO} - V_2\right)^{1/2} \quad . \tag{B-5}$$

Equations (B-1) and (B-5) can be solved for the diffusion potential V_{BO}, yielding

$$V_{BO} = \varphi_{ms} + V_1/2 - V_1^{1/2}\left(\varphi_{ms} + V_1/4 - V_2\right)^{1/2} \quad . \tag{B-6}$$

Equation (B-6) reduces to φ_{ms} if no interfacial layer is present ($\delta = 0$). Referring to Eq. (B-2), this is the usual result for a simple metal-semiconductor contact with no surface states.[36]

When a reverse bias V is applied to the junction, the band diagram appears as in Fig. B-7. The potential rise, V_B, in the semiconductor and the voltage, Δ, across the interfacial layer are, in

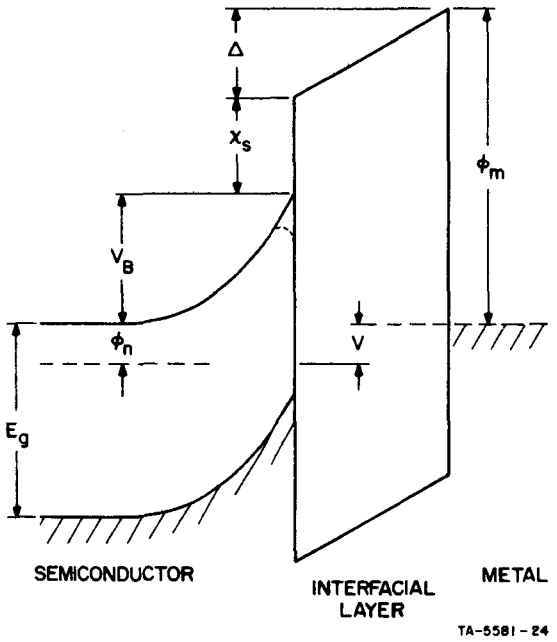

FIG. B-7 MOS CONTACT OF FIG. B-6 WITH APPLIED REVERSE BIAS V

general, different from their equilibrium values (V_{BO} and Δ_o, respectively). Equations (B-1) and (B-5), respectively, are now replaced by

$$\varphi_{ms} + V = V_B + \Delta \qquad \text{(B-7)}$$

and

$$\Delta = V_1^{1/2}(V_B - V_2)^{1/2} \quad . \qquad \text{(B-8)}$$

By eliminating Δ between these two equations we obtain

$$\varphi_{ms} + V = V_B + V_1^{1/2}(V_B - V_2)^{1/2} \quad . \qquad \text{(B-9)}$$

The space charge Q_{sc} in the semiconductor is given by

$$Q_{sc} = [2e\epsilon_s N_D(V_B - V_2)]^{1/2} \quad , \tag{B-10}$$

and the differential capacitance C, per unit area, by

$$C = \partial Q_{sc}/\partial V = (2e\epsilon_s N_D)^{1/2}(\partial/\partial V)[(V_B - V_2)^{1/2}] \quad . \tag{B-11}$$

By solving Eq. (B-9) for $(V_B - V_2)^{1/2}$ and performing the differentiation indicated in Eq. (B-11), C is obtained as

$$C = (e\epsilon_s N_D/2)^{1/2}(\varphi_{ms} + V + V_1/4 - V_2)^{-1/2} \quad . \tag{B-12}$$

Squaring and inverting Eq. (B-12) yields

$$1/C^2 = (2/e\epsilon_s N_D)(\varphi_{ms} + V + V_1/4 - V_2) \quad . \tag{B-13}$$

The magnitude V_o of the intercept of this relation on the V-axis is given by

$$V_o = \varphi_{ms} + V_1/4 - V_2 \quad . \tag{B-14}$$

If Δ_o in Eq. (B-1) is replaced by Eq. (B-5) and the resulting expression for φ_{ms} is substituted into Eq. (B-14), we obtain

$$V_o = V_{BO} - V_2 + V_1/4 + (V_1 V_{BO})^{1/2} \quad . \tag{B-15}$$

Except for the notation and the presence of the reserve layer term, this expression is identical to Eq. (21) of Ref. 14. Upon the substitution of Eq. (B-4) for V_1, Eq. (B-14) gives the explicit dependence of the $1/C^2$ vs. V intercept on interfacial layer thickness δ.

Figure B-8 shows a plot of V_o and V_{BO} vs. δ, where the parameters ϵ_s, N_D, φ_m, χ_s, and φ_n are chosen to correspond to the Au/GaP

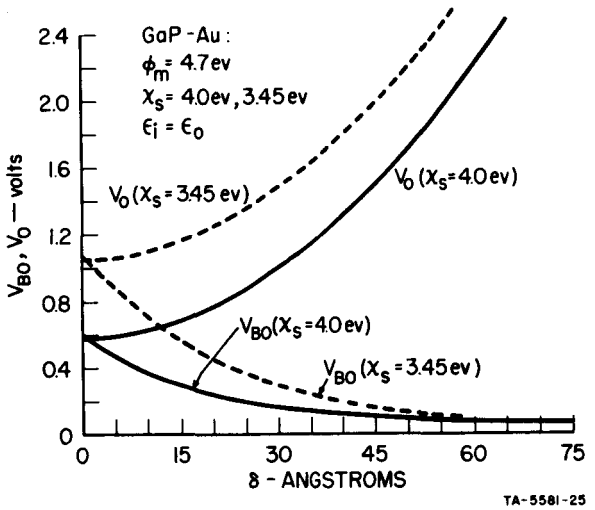

FIG. B-8 DIFFUSION POTENTIAL AND $1/C^2$ INTERCEPT vs. INTERFACIAL LAYER THICKNESS FOR GaP–Au DIODE, ASSUMING MOS MODEL WITHOUT SURFACE STATES (SEC. 3a, Appendix B)
Curves calculated on the basis of χ_s = 4.0 ev are shown as solid lines; dashed lines indicate χ_s = 3.45 ev.

contacts described in Sec. 2 of this appendix. The dielectric constants ϵ_i of the interfacial layer is taken to be that of vacuum. The behavior of V_o and V_{BO} with δ, as depicted in Fig. B-8, is immediately seen to be incompatible with the experimental observations outlined in Sec. I, the main discrepancy being the rapid decrease in V_{BO} with increasing δ; a decrease in V_{BO} is not observed experimentally. The magnitude of V_{BO} for thin layers ($\delta < 10$ Å) for $\chi_s \simeq 4.0$ eV is also seen to be in disagreement with the measured value for Au/GaP contacts (~ 1.3V). This could be attributed to the fact that in this case the values taken for χ_s was only an estimate.[18] A recently measured value of χ_s for the cleaved GaP (110) surface is 3.45 eV.[37] Use of this value in computing V_{BO} for Fig. B-8 results in $V_{BO} \simeq 1.15$ eV, which is closer to the measured value. As shown by the dashed lines in Fig. B-8, however, the behavior of V_o and V_{BO} is still in disagreement with experiment.

We proceed in the next section to analyze the bias behavior of an MOS contact which incorporates a simple surface states model. The

same model has been successful in accounting for the variation of the barrier height with metal work function in GaP and Si contacts.[18]

b. MOS Contact with Surface States; Thin Interfacial Layer

The presence of semiconductor surface states in the MOS diode can be accounted for by Bardeen's simple model,[29] which assumes that surface states are uniformly distributed in energy over an energy interval in the semiconductor forbidden gap. The density is taken to be D_s states/cm^2/eV, and filling the states up to some energy, denoted by φ_o, results in a neutral surface. The energy φ_o lies in the forbidden gap and is measured from the valence band edge.

Equations (B-1) and (B-7) of Sec. 3a are evidently still valid for the present model. Gauss's law for the potentials across the interfacial layer, with and without bias, respectively, yields

$$\Delta = V_1^{1/2}\left(V_B - V_2\right)^{1/2} + \left(\delta/\epsilon_i\right)Q_{ss}(V) \quad , \tag{B-16}$$

and

$$\Delta_o = V_1^{1/2}(V_{BO} - V_2)^{1/2} + (\delta/\epsilon_i)Q_{ss}(0) \quad , \tag{B-17}$$

where $Q_{ss}(V)$ and $Q_{ss}(0)$ denote, respectively, the charge in surface states with and without bias V.

For zero bias, $Q_{ss}(0)$ can be written in the 0°K approximation as[18]

$$\begin{aligned} Q_{ss}(0) &= -eD_s(E_F - \varphi_o) \\ &= -eD_s(E_g - V_{BO} - \varphi_o - \varphi_n) \quad . \end{aligned} \tag{B-18}$$

Using the definition

$$\alpha = eD_s\,\frac{\delta}{\epsilon_i} \quad , \tag{B-19}$$

we can write Eq. (B-17) as

$$\Delta_o = V_1^{1/2}(V_{BO} - V_2)^{1/2} - \alpha(E_g - V_{BO} - \varphi_o - \varphi_n) \quad . \qquad (B\text{-}20)$$

Solving Eqs. (B-1) and (B-20) for V_{BO}, we obtain

$$V_{BO} = [\varphi_{ms} + \alpha(E_g - \varphi_o - \varphi_n)]/(1 + \alpha) + \tfrac{1}{2}V_1/(1 + \alpha)^2$$

$$- V_1^{1/2}\{[1 + \alpha][\varphi_{ms} + \alpha(E_g - \varphi_o - \varphi_n)] + \tfrac{1}{4}V_1\}^{1/2}/(1 + \alpha)^2 \quad . \qquad (B\text{-}21)$$

When a bias is applied to the junction, an assumption must be made regarding the behavior of the charge Q_{ss} in surface states. For a very thin interfacial film, it is expected that the Fermi level E_F at the semiconductor surface will remain "pinned" to the metal Fermi level when a bias is applied.[24] The change in position of the Fermi level at the semiconductor surface relative to the semiconductor energy bands is therefore $\Delta - \Delta_o$, and the change in surface states charge is given by

$$\Delta Q_{ss} = -eD_s(\Delta - \Delta_o) \quad , \qquad (B\text{-}22)$$

where $\Delta Q_{ss} = Q_{ss}(V) - Q_{ss}(0)$.

If Eq. (B-17) is subtracted from Eq. (B-16), we obtain

$$\Delta - \Delta_o = V_1^{1/2}[(V_B - V_2)^{1/2} - (V_{BO} - V_2)^{1/2}] + \frac{\delta}{\epsilon_i}\Delta Q_{ss} \quad . \qquad (B\text{-}23)$$

Using Eqs. (B-19) and (B-22), we can rewrite this as

$$(1 + \alpha)(\Delta - \Delta_o) = V_1^{1/2}[(V_B - V_2)^{1/2} - (V_{BO} - V_2)^{1/2}] \quad . \qquad (B\text{-}24)$$

Subtraction of Eq. (B-1) from Eq. (B-7) results in

$$V = V_B - V_{BO} + \Delta - \Delta_o \quad . \qquad (B\text{-}25)$$

If $\Delta - \Delta_o$ is eliminated between Eqs. (B-24) and (B-25), we obtain, after rearrangement,

$$V_1^{1/2}(V_{BO} - V_2)^{1/2} + (1 + \alpha)V_{BO} = V_1^{1/2}(V_B - V_2)^{1/2} - (1 + \alpha)(V - V_B) \quad . \tag{B-26}$$

Combining Eqs. (B-1) and (B-20) yields the expression

$$V_1^{1/2}(V_{BO} - V_2)^{1/2} + (1 + \alpha)V_{BO} = \varphi_{ms} + \alpha(E_g - \varphi_o - \varphi_n) \quad . \tag{B-27}$$

The right hand sides of Eqs. (B-26) and (B-27) are evidently equal, therefore we can write

$$V_1^{1/2}(V_B - V_2)^{1/2} - (1 + \alpha)V + (1 + \alpha)(V_B - V_2) = \varphi_{ms} + \alpha(E_g - \varphi_o - \varphi_n) - (1 + \alpha)V_2 \quad . \tag{B-28}$$

where $(1 + \alpha)V_2$ has been subtracted from both sides of Eq. (B-28).

In calculating the capacitance of the contact, we find the differential charge dQ which flows into one connection to the contact when the bias voltage is changed by dV. Charge which flows in and out of surface states is evidently supplied by the metal, in this case, owing to the assumption that the Fermi level at the semiconductor surface is pinned to the metal Fermi level. All charge flowing into the semiconductor from the external circuit therefore resides in the space charge layer, and to calculate capacitance, we need only differentiate the semiconductor space charge Q_{sc} with respect to applied voltage V. This is easily done by first solving Eq. (B-28) for $(V_B - V_2)^{1/2}$:

$$(V_B - V_2)^{1/2} = -\frac{1}{2} V_1^{1/2}/(1 + \alpha) + \{[\varphi_{ms} + \alpha(E_g - \varphi_o - \varphi_n)]/(1 + \alpha) + \frac{1}{4} V_1/(1 + \alpha)^2 + V - V_2\}^{1/2} \quad . \tag{B-29}$$

The differential capacitance C is found from Eq. (B-11); squaring and inverting C, we obtain

$$1/C^2 = (2/e\epsilon_s N_D)\{[\varphi_{ms} + \alpha(E_g - \varphi_o - \varphi_n)]/(1 + \alpha) + \frac{1}{4} V_1/(1 + \alpha)^2 + V - V_2\} \quad . \tag{B-30}$$

The V-axis intercept is given by

$$V_o = [\varphi_{ms} + \alpha(E_g - \varphi_o - \varphi_n)]/(1 + \alpha) + \frac{1}{4} V_1/(1 + \alpha)^2 - V_2 \quad . \tag{B-31}$$

Equations (B-21) and (B-31) have been plotted as functions of δ in Fig. B-9. The semiconductor and interfacial layer parameters have been chosen to correspond to the GaP/Au junction, as in Fig. B-8. The V-axis intercept V_o follows V_{BO} closely over the entire range of δ shown here, indicating that for the range of validity of this model, the $1/C^2$ intercept is an accurate measure of the diffusion potential. Referring to Table B-1 and Figs. B-4 and B-5, we can see that the model does appear

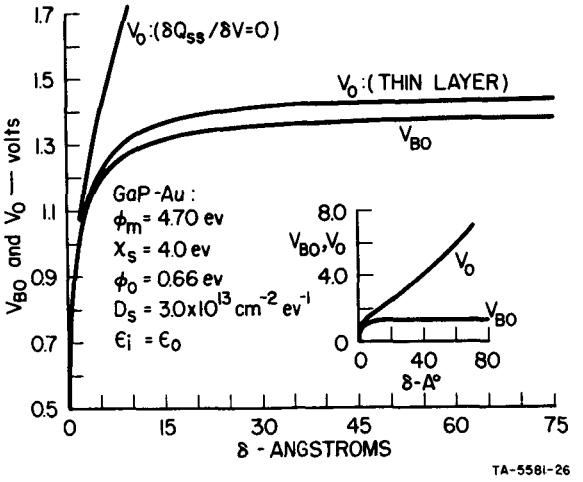

FIG. B-9 DIFFUSION POTENTIAL AND $1/C^2$ INTERCEPT vs. INTERFACIAL LAYER THICKNESS FOR GaP–Au DIODE ACCORDING TO MODELS DESCRIBED IN SECS. 3b AND 3c (MOS MODEL WITH SURFACE STATES)
The inset shows a larger portion of the variation of V_o with δ for the assumption of $\partial Q_{ss}/\partial V = 0$ (Sec. 3c)

to provide a correct description of the GaP/Au contact for the thinnest interfacial layers. As film thickness increases, it is expected that the assumptions leading to Eq. (B-22) will not be valid and a new model must be used. The model considered in the next section neglects entirely the change in surface states charge with bias.

c. MOS Contact; $\partial Q_{ss}/\partial V = 0$

The assumption will be made here that the surface charge Q_{ss} remains constant at its equilibrium value $Q_{ss}(0)$ when a bias is applied. For a contact whose diffusion potential V_{BO} is strongly "pinned" by surface states, this is clearly not an a priori reasonable assumption; but it will be seen that the model does, nevertheless, provide an expression for V_o which has some of the features required to explain the experimental data for GaP.

Referring to Eqs. (B-16) and (B-17), we see that $Q_{ss}(0)$ and $Q_{ss}(V)$ are equal for the present model; subtraction of Eq. (B-17) from Eq. (B-16) therefore yields

$$\Delta - \Delta_o = V_1^{1/2}[(V_B - V_2)^{1/2} - (V_{BO} - V_2)^{1/2}] \quad . \tag{B-32}$$

Equation (B-25) is still valid for this case, and Eqs. (B-32) and (B-25) can be solved for $(V_B - V_2)^{1/2}$, yielding

$$(V_B - V_2)^{1/2} = -\frac{1}{2} V_1^{1/2} + \left[\frac{1}{4} V_1 + V_1^{1/2}(V_{BO} - V_2)^{1/2} + V_{BO} - V_2 + V\right]^{1/2} \quad . \tag{B-33}$$

Using Eq. (B-11) to find C, we finally obtain for $1/C^2$,

$$1/C^2 = (2/e\epsilon_s N_D)\left[V_{BO} + V - V_2 + V_1^{1/2}(V_{BO} - V_2)^{1/2} + \frac{1}{4} V_1\right] \quad . \tag{B-34}$$

The intercept is evidently given by

$$V_o = V_{BO} + V_1^{1/2}(V_{BO} - V_2)^{1/2} + \frac{1}{4} V_1 - V_2 \quad . \tag{B-35}$$

Equation (B-35) is plotted vs. δ in Fig. B-9 for the GaP/Au diode. The intercept V_o is now observed to diverge rapidly for $\delta > 5$ Å, while V_{BO} does not change appreciably after δ reaches 5 Å or so. This is in qualitative agreement with experiment, but a closer examination reveals that the predicted difference in V_{BO} and V_o is too large for the thinnest interfacial layers ($\delta \simeq 5$ Å). Accordingly, we attempt in the next section to correct this discrepancy by providing for a transition from the model of Sec. 3b to the present model.

d. Model for Thicker Interfacial Layers

The assumption $\partial Q_{ss}/\partial V \approx 0$ made in the last section could be valid only for some accidental combination of junction parameters which would allow the Fermi level at the semiconductor surface to remain fixed with respect to the semiconductor energy bands as a bias is applied. A more realistic assumption is to allow Q_{ss} to change in proportion to changes in the potential across the interfacial layer, as was done in Sec. 3b. In this case, however, a smaller constant of proportionality will be chosen, to correspond to the fact E_F at the semiconductor surface is not pinned to E_F in the metal. Accordingly, instead of Eq. (B-22) we will write

$$\Delta Q_{ss} = -\lambda e D_s(\Delta - \Delta_o) \quad , \qquad (B\text{-}36)$$

where $0 \leq \lambda \leq 1.0$. The parameter λ is expected to be a function of interfacial layer thickness δ, ranging from 1.0 for small values of δ (corresponding to Sec. 3b) to zero for some intermediate value of δ. It is obvious that an equation of the form of Eq. (B-36) cannot correctly describe the variation in ΔQ_{ss} with bias for very thick interfacial layers; for very thick layers, E_F at the surface of the semiconductor coincides with the bulk Fermi level, as is usually the case in field-effect conductivity experiments.[37] It can be verified that this condition leads to the expression

$$\Delta Q_{ss} = eD_s V - eD_s(\Delta - \Delta_o) \quad . \qquad (B\text{-}37)$$

Use of Eq. (B-37) to calculate capacitance leads to an expression for $1/C^2$ which is linear in V only if one assumes a measurement signal frequency much larger than the reciprocal of the time constant associated with transfer of charge between the bulk semiconductor and surface states. The expression derived is as follows:

$$1/C^2 = \left[2(1 + \alpha)/e\epsilon_s N_D\right]\left[(1 + \alpha)(V_{BO} - V_2) + V_1^{1/2}(V_{BO} - V_2)^{1/2} + V + \frac{1}{4} V_1/(1 + \alpha)\right] , \quad \text{(B-38)}$$

It can be verified that in the limit of very large δ, Eq. (B-38) becomes δ^2/ϵ_i^2, the reciprocal square of the geometrical capacitance of the interfacial layer. Equation (B-38) has the correct qualitative behavior regarding V-axis intercept; the intercept increases rapidly with δ. However, the slope is too large, becoming much greater than $2/e\epsilon_s N_D$ for relatively small values of δ. This is not in accordance with experiment, and consequently this model is rejected.

Returning to the original subject of this section, we will proceed to calculate capacitance based on Eq. (B-36). If we continue to assume, as in Sec. 3b, that changes in Q_{ss} are due entirely to charge transfer between the metal and surface states, then Eq. (B-11) is still valid for deriving the capacitance relation.

Using Eqs. (B-23), (B-25), and (B-36), we can derive the expression for $(V_B - V_2)^{1/2}$ as

$$(V_B - V_2)^{1/2} = -\frac{1}{2} V_1^{1/2}/(1 + \alpha\lambda) + \left[\frac{1}{4} V_1/(1 + \alpha\lambda)^2 + V + V_{BO} - V_2 + V_1^{1/2}(V_{BO} - V_2)^{1/2}/(1 + \alpha\lambda)\right]^{1/2} . \quad \text{(B-39)}$$

Using Eq. (B-11), we can calculate the capacitance from Eq. (B-39); the $1/C^2$ vs. V relation is obtained as

$$1/C^2 = (2/e\epsilon_s N_D)\left[V + V_{BO} - V_2 + V_1^{1/2}(V_{BO} - V_2)^{1/2}/(1 + \alpha\lambda) + \frac{1}{4} V_1/(1 + \alpha\lambda)^2\right] . \quad \text{(B-40)}$$

The intercept V_o is evidently given by

$$V_o = V_{BO} + V_1^{1/2}(V_{BO} - V_2)^{1/2}/(1 + \alpha\lambda) + \frac{1}{4} V_1/(1 + \alpha\lambda)^2 - V_2 . \quad \text{(B-41)}$$

An important feature of the variation of Q_{ss} with V specified in Eq. (B-36) is that it produces a linear $1/C^2$ vs. V relation [Eq. (B-40)], in agreement with the observed $1/C^2$ behavior for GaP diodes.

As discussed earlier, we shall require that λ depend on δ in such a way as to provide a transition from the model of Sec. 3b to that of Sec. 3c as δ increases. Since the exact dependence of λ on δ is not known, an arbitrary function will be chosen such that

$$\begin{aligned} \lambda(\delta) &= 1.0 \qquad \delta = 0 \\ \lambda(\delta) &\to 0 \qquad \delta > \delta_o \end{aligned} \quad \text{(B-42)}$$

where δ_o is some value of δ that will be chosen arbitrarily to provide a reasonable fit to the experimental observations. An equation which has the features specified in Eq. (B-42) is

$$\lambda(\delta) = \{1 + \exp[\beta(\delta - \delta_o)]\}^{-1} , \quad \text{(B-43)}$$

where β is chosen to provide the desired rapidity of the transition from $\lambda = 1.0$ to $\lambda \approx 0$. Again, β is arbitrary, since the actual variation of λ with δ is not known. Figure B-10 shows a plot of V_o vs. interfacial layer thickness δ, and was derived using Eq. (B-41) and allowing λ to vary according to Eq. (B-43). Here β and δ_o are arbitrarily chosen to

be 1.0 $\mathring{A}^{-1}$ and 10 $\mathring{A}$, respectively. The metal-semiconductor parameters are chosen to correspond to GaP/Au contacts, and V_{BO} calculated from Eq. (B-21) is plotted for comparison, as in Fig. B-9. The variation of V_o with δ is now seen to be consistent with the observed behavior of the GaP diodes. For thin interfacial layers, V_o and V_{BO} agree closely within experimental accuracy, and for thicker layers, V_o diverges rapidly, while V_{BO} remains relatively unchanged. The exact shape of the V_o curve is of course determined by the arbitrary function, Eq. (B-43), which must simply be regarded as a convenient device for providing a smooth transition between the "thin layer" and "thick layer" regimes.

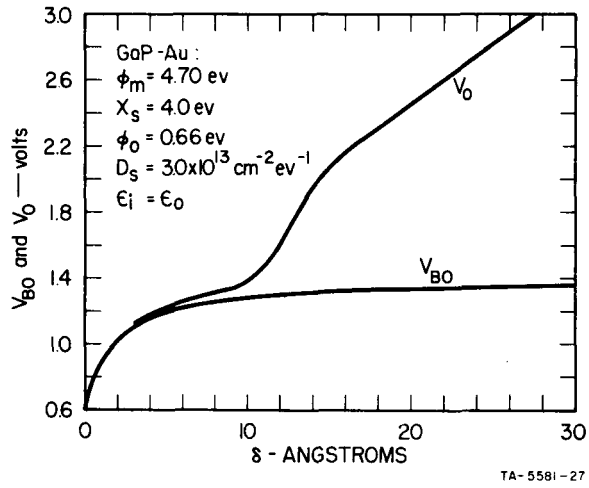

FIG. B-10 VARIATION OF V_{BO} AND V_o WITH INTERFACIAL LAYER THICKNESS δ FOR GaP-Au DIODE ACCORDING TO MODEL OF SEC. 3d
This model provides for a gradual transition from the model of Sec. 3b to the model of Sec. 3c at $\delta \simeq 10$ Å

4. Discussion

The model of Sec. 3d has been shown to provide a reasonable explanation for the observed variation of V_o and V_{BO} for n-type GaP/metal surface barrier diodes. The most important features of the observed $1/C^2$ vs. V data are

1. The linearity of the curves
2. The fact the slopes seem to be related to the donor density in the usual way, independent of interfacial layer thickness and
3. the fact large increases in the V-axis intercept are correlated with increases in interfacial layer thickness.

The proposed model is consistent with all of these observations. The model also explains both the fact that V_o and V_{BO} agree closely for diodes where the interfacial film thickness was held to a minimum, and the fact that V_{BO}, as determined photoelectrically, does not vary significantly with changes in interfacial film thickness.

The models postulated in Secs. 3b and 3d require that the Fermi level at the semiconductor surface move up and down through a uniform surface states distribution in the forbidden gap as the applied voltage is varied. A calculation has been made, showing that for the highest values of reverse bias, the maximum displacement of the Fermi level from its equilibrium position at the semiconductor surface is about 0.1 volt. Thus, strictly speaking, the surface state density need only be uniform (D_s = Constant) over about 0.1 volt in the forbidden gap in order for the proposed models to be valid for reverse bias. High values of forward bias produce considerably larger displacements in the Fermi level at the semiconductor surface; if the Fermi level enters a region of the surface state density which is not uniform, then the $1/C^2$ vs. V curve will deviate from a straight line. Such deviations from a straight line have been observed in the $1/C^2$ vs. V curves for forward bias. The $1/C^2$ plot usually bends upward as forward bias is increased, but occasionally a downward bending is observed. This behavior is difficult to reproduce, and limitations on the capacitance measuring equipment usually prevent the taking of data for forward bias greater than $\sim$ 0.7 V; consequently, this effect has not been thoroughly investigated.

The possibility that the MOS model without surface states is in fact a more nearly correct model for GaP-metal has also been considered. Suppose one actually measures φ_m (Fig. B-6) in a photothreshold measurement; i.e., the interfacial layer is not transparent to photoelectrons.

The metal work function φ_m is not the vacuum work function φ_m (vac). A simple model gives the effective work function of the metal-insulator interface as $\varphi_m = \varphi_m(\text{vac}) - \chi_i$, where χ_i is the electron affinity of the insulating interfacial layer.[39] To a first-order approximation, φ_m does not vary with δ; this would account for the constancy of the photothreshold with δ. The $1/C^2$ intercept also has the correct qualitative behavior with changes in δ (Fig. B-8). This model is rejected for the reasons given in the following paragraphs.

First, the voltage-current characteristics for GaP-metal diodes (e.g., GaP-Au) indicate that the mechanism of current flow in these diodes is thermionic emission over a parabolic (Schottky) barrier. This observation gives good reason to believe that photoelectrons, as well as thermal electrons, tunnel freely through the interfacial layer; i.e., the interfacial layer, at least for well cleaned substrates (Sec. II), is transparent to electrons whose energy exceeds the potential barrier height. Referring to Fig. B-8, it is observed that V_{BO} changes very rapidly for relatively small changes in δ, in the region of $\delta \approx 5$ Å for the MOS model without surface states. In view of the transparency of the interfacial layer to electrons, as discussed above, one should easily be able to observe this change in the photothreshold measurements. In the experiments reported here, however, the change is not observed.

Second, the MOS model without surface states, again referring to Fig. B-8, predicts a large difference between V_{BO} and V_o, even for very small δ (~ 5 Å). One certainly expects the interfacial layer to be transparent to electrons for these thicknesses; hence, photothreshold measurements should yield the barrier height φ_{Bn} (equal to V_{BO} within a few mV for the present experiments), and the value of V_o from capacitance measurements should exceed V_{BO} by several tenths of a volt. On the contrary, the experiments show V_o and V_{BO} to be practically equal for diodes prepared in the Vac-Ion system using etched and protected GaP substrates.

The variation of V_{BO} with φ_m for GaP-metal diodes is also not explained by an MOS structure without surface states; the assumption of a relatively high density of surface states, on the other hand, provides a reasonable explanation for the experimental V_{BO} vs. φ_m data.[18]

APPENDIX C

RESERVE LAYER CORRECTION FOR INCOMPLETE DONOR IONIZATION

APPENDIX C

RESERVE LAYER CORRECTION FOR INCOMPLETE DONOR IONIZATION

The reserve layer correction V_2, which is introduced in Sec. 3a of Appendix B, arises from the presence of mobile carriers at the edge of the depletion region. This term is derived by Goodman[14] for the case of completely ionized donors. Since the donor levels in GaP are relatively deep (0.07 - 0.08 eV),[34,40] the donors will not be completely ionized at room temperature. We will denote the fraction of ionized donors by η, and will assume that the Fermi level is always more than kT/e eV below the bottom of the conduction band. The charge density ρ in the semiconductor depletion layer can then be written

$$\rho(x) = +eN_D \left[\frac{1}{1 + (1/\eta - 1) \exp(-e\psi/kT)} - \eta \exp(-e\psi/kT) \right] , \quad \text{(C-1)}$$

where x is the distance into the semiconductor measuring from the surface, and ψ is the potential energy in eV of an electron measured from the bottom of the conduction band in the bulk semiconductor. The potential energy ψ is a function of x, and at the surface with no applied bias, $\psi = V_{BO}$. According to the convention introduced in Sec. 3 of Appendix B, $\psi = V_{BO}$ at the surface when a bias is applied. In terms of Eq. (C-1), Poisson's equation for the depletion layer may be written:

$$\frac{d^2\psi}{dx^2} = \frac{eN_D}{\epsilon_s} \left[\frac{1}{1 + (1/\eta - 1) \exp(-e\psi/kT)} - \eta \exp(-e\psi/kT) \right] . \quad \text{(C-2)}$$

Integration of this equation once subject to the boundary conditions $\psi = 0$, $d\psi/dx = 0$, yields

$$\frac{d\psi}{dx} = -\frac{2kT\, N_D^{1/2}}{\epsilon_s} \{ \ell n[\eta \exp(e\psi/kT) + 1 - \eta] + \eta \exp(-e\psi/kT) - \eta \}^{1/2}$$

$$\simeq -(2kT\, N_D/\epsilon_s)\, [e\psi/kT - (\eta - \ell n\, \eta)]^{1/2} , \quad \psi \gg \frac{kT}{e} . \quad \text{(C-3)}$$

Gauss's law states the electric field at the semiconductor surface, E_s, is related to the space charge Q_{sc} by

$$Q_{sc} = - \epsilon_s E_s \text{ coul/cm}^2 \quad . \qquad \text{(C-4)}$$

The electric field at the semiconductor surface is given by

$$E_s = \left(\frac{d\psi}{dx}\right)_s \quad , \qquad \text{(C-5)}$$

where subscript "s" denotes the value of a variable at the surface. The space charge can therefore be expressed as

$$Q_{sc} \simeq (2e \epsilon_s N_D)^{1/2} [\psi_s - (\eta - \ell n \eta) kT/e]^{1/2} \quad , \qquad \text{(C-6)}$$

using Eqs. (C-3), (C-4), and (C-5). Since $\psi_s = V_B$, Eq. (C-6) leads to the result

$$Q_{sc} = (2e \epsilon_s N_D)^{1/2} (V_B - V_2)^{1/2} \quad , \qquad \text{(C-7)}$$

where

$$V_2 = (\eta - \ell n \eta) kT/e \quad . \qquad \text{(C-8)}$$

For the GaP crystals described in the present work, it is estimated that slightly more than half of the donors are ionized, and this leads to a value of ~ 0.03 eV for V_2 at room temperature. This value differs insignificantly from the usual result for the complete donor ionization which is $V_2 = kT/e = 0.026$ eV at room temperature.[14] At lower temperatures or higher doping levels, the difference could be significant.

REFERENCES

1. D. V. Geppert, "Research on Cold Cathodes," First Quarterly Report, Contract NAS 5-9581, SRI Project 5511, Stanford Research Institute, Menlo Park, California (August 1960).

2. R. Suhrman and G. Wedler, Zeits. für Angew. Physik 14, p. 70 (1962).

3. G. E. Moore and H. W. Allison, Phys. Rev. 77, p. 246 (1950).

4. T. S. Kirsanova, A. R. Shul'man, and A. V. Dement'eva, Soviet Phys. Solid State 4, p. 1918 (March 1963).

5. D. V. Geppert and B. V. Dore, "Photoconductor-Semiconductor Emitters," First Quarterly Report, Contract Da-44-009 AMC-1206(T), SRI Project 5581, Stanford Research Institute, Menlo Park, California (October 1965).

6. P. N. Russell and A. S. Eisenstein, Jour. Appl. Phys. 25, 8, pp. 954-961 (August 1954).

7. B. J. Hopkins and K. J. Ross, Jour. Appl. Phys. 34, 7, pp. 2111-2112 (July 1963).

8. Sin-ichiro Narita, Jour. Phys. Soc. Japan 9, 1, pp. 22-27 (January-February 1954).

9. J. V. Florio, Jour. Appl. Phys. 34, 1, pp. 200-206 (January 1963).

10. T. S. Kirsanova and A. R. Shul'man, Soviet Physics-Solid State 6, 1, pp. 225-230 (July 1964).

11. Yu G. Ptushinskii, Radiotek. Elektronika 5, 10, pp. 1663-1668 (1960).

12. J. E. Dueker and G. B. Hensley, Phys. Rev. 136, p. 9190 (5 October 1964).

13. M. L. Report No. 1324, Microwave Laboratory, Stanford University, Stanford, California (unpublished report).

14. A. M. Goodman, J. Appl. Phys. 34, 329 (1963).

15. W. Shockley and G. L. Pearson, Phys. Rev. 74, 232 (1948).

16. H. C. Montgomery and W. L. Brown, Phys. Rev. 103, 865 (1956).

17. A. M. Cowley and H. Heffner, J. Appl. Phys. 35, 255 (1964).

18. A. M. Cowley and S. M. Sze, J. Appl. Phys. 36, 3212, (October 1965).

19. J. J. Scheer and J. Van Laar, Solid State Comm. 3, p. 189 (1965).

20. R. J. Ackerman and R. J. Thorn, Progress in Ceramic Science 1, p. 51 ff (1965).

21. B. P. Nikonov and N. G. Otmakhova, Zhur. Fiz. Khim. 35, pp. 1494-1498 (1961).

22. G. H. Metson, Proc. Inst. Elect. Engrs. (London) 110, pp. 845-847 (1963).

23. M. G. Inghram and J. Drowart, "Mass Spectrometry Applied to High Temperature Chemistry," Proceedings International Symposium on High Temperature Technology, Asilomar Conference Grounds, California, October 1959 (McGraw Hill, 1960), pp. 219-240.

24. R. J. Archer and M. M. Atalla, Ann. N.Y. Acad. Sci. 101, 697 (1963).

25. H. G. White and R. A. Logan, J. Appl. Phys. 34, 1990 (1963).

26. W. G. Spitzer and C. A. Mead, J. Appl. Phys. 34,3061 (1963).

27. A. M. Goodman, Surface Science 1, 54 (1964).

28. A. M. Goodman, J. Appl. Phys. 35, 573 (1964).

29. J. Bardeen, Phys. Rev. 71, 717 (1947).

30. C. J. Frosch and L. Derick, J. Electrochem. Soc. 108, 251 (1961).

31. C. Hilsum and A. C. Rose-Innes, Semiconducting III-V Compounds (Pergamon Press, New York, 1961) p. 8.

32. D. Kahng [Bell Syst. Tech. Jour. 43, 215 (1964)] has reported similar observations in GaAs/Au Schottky barrier diodes.

33. Hilsum and Rose-Innes, op. cit., p. 122.

34. Ibid., p. 80.

35. L. L. Chang and G. L. Pearson, J. Phys. Chem. Solids 25, 23 (1964).

36. H. K. Henisch, Rectifying Semiconductor Contacts (Oxford University Press, New York, 1957), Chap. 7.

37. T. E. Fischer, Bell Telephone Laboratories, Inc., Murray Hill, New Jersey (private communication).

38. See for example W. Schockley and G. L. Pearson, Phys. Rev. 74, 232 (1948); also H. G. Montgomery and W. L. Brown, Phys. Rev. 103, 865 (1956).

39. N. F. Mott, R. W. Gurney, Electronic Processes in Ionic Crystals, (Oxford, London, 1940), p. 169.

40. C. J. Frosch, M. Gershenzon, D. F. Gibbs, Symposium on "Preparation of Single Crystals of the III-V Compounds," Battelle Memorial Institute, Columbus, Ohio (November 1959).